cultured without the FMS/PA6-P cells (the non-co-cultured group) (6/6). However, as shown in Figure 2A, the proportion of human CD45$^+$ cells, CD34$^+$ cells and CD34$^+$CD38$^-$ cells was significantly higher in the BM of the co-cultured group than in the BM of the non-co-cultured group. In the BM of the co-cultured group, mature human myeloid cells (CD14$^+$: 0.57%), B cells (CD19$^+$: 0.18%), erythroid cells (CD235a$^+$: 3.31%) and megakaryocytic cells (CD41$^+$: 0.21%) were also detected. A clear difference between both groups was also seen in human CD45$^+$ cells in the peripheral blood (Figure 2A). Figure 2B shows a representative flow cytometric pattern (CD45/CD34 and CD38/CD34 stains) of BM cells from the SCID mice that received L$^-$CBMC cultured with or without FMS/PA6-P cells.

The presence of human cells was further proven in the SCID mice of the co-cultured group by PCR analysis using the human-specific DNA 17α-satellite gene; four out of five mice showed human DNA in their BM (Figure 2C). In contrast, no human DNA was detected in the non-co-cultured group. Even in those mice showing human DNA in their BM, we failed to detect human DNA in the peripheral blood of the animals, implying that human-type cells were under the detection level of PCR in the peripheral blood in contrast to the BM.

These findings indicate that HSC and progenitor cells contained in the culture-expanded cells homed to the BM, where they proliferated and differentiated into multi-lineage mature blood cells, suggesting that the FMS/PA6-P cells provide a suitable microenvironment for the proliferation of functional HSC and progenitor cells.

As mentioned above, we observed a decline in CFU-C counts after trypsin-EDTA treatment. The cells transplanted into the SCID mice were collected from the co-culture using trypsin-EDTA treatment, and it is possible that this treatment might damage the *in vivo* proliferation and differentiation activity of the transplanted cells.

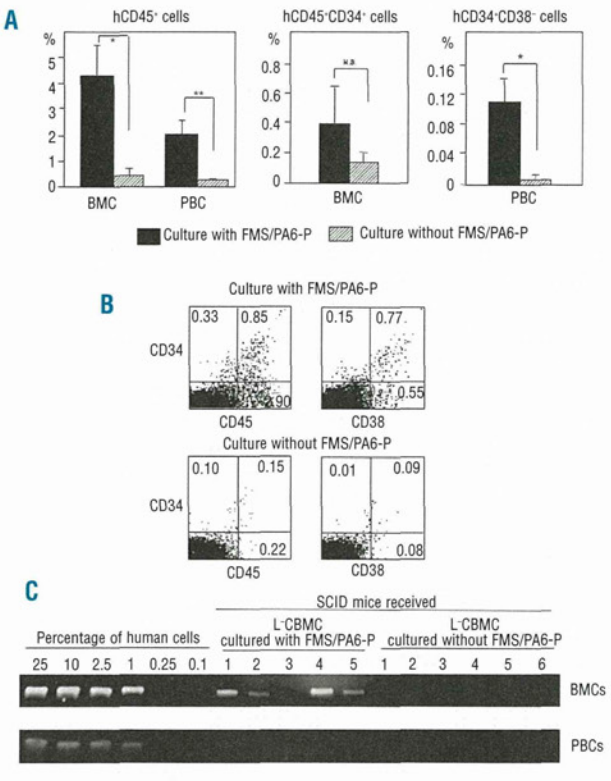

Figure 2. Reconstitution of human cells in SCID mice that received culture-expanded L$^-$CBMC. (A) Higher engraftment of human cells in SCID mice that received L$^-$CBMC co-cultured with FMS/PA6-P cells. The L$^-$CBMC were cultured in a 12-well plate with the FMS/PA6-P cells for 2 weeks and all cells in one well, including the FMS/PA6-P cells and hematopoietic cells, were harvested and injected into a single SCID mouse via the intravenous route. All cells in one well, cultured without the FMS/PA6-P cells, were also collected and injected into a single SCID mouse. Eight weeks after the transplantation, BM and peripheral blood cells were collected and the percentages of human CD45$^+$ cells, CD34$^+$ cells and CD34$^+$CD38$^-$ cells were measured using FACScan. **P<0.01; *P<0.05. (B) Representative flow cytometric pattern of BM cells from SCID mice that received L$^-$CBMC cultured with or without FMS/PA6-P cells. BM cells collected from the SCID mice were double-stained with anti-human CD45 and anti-human CD34 monoclonal antibodies or with anti-human CD38 and anti-human CD34 monoclonal antibodies and analyzed by a FACScan. The values indicate the percentages of the population in whole BM cells. (C) Detection of human DNA in SCID mice that received L$^-$CBMC co-cultured with FMS/PA6-P cells. Four of five mice, transplanted with the expanded cells produced in the co-culture of L$^-$CBMC with FMS/PA6-P cells, contained human DNA in the BM, whereas no human DNA was detected in the BM of six mice transplanted with the expanded cells produced in culture of L$^-$CBMC without FMS/PA6-P cells.

Contribution of neural cell adhesion molecules to the human hematopoiesis-supporting ability of FMS/PA6-P cells

Since many studies have demonstrated that stromal cell-hematopoietic cell interactions in the marrow microenvironment are crucial for physiological hematopoiesis, we next investigated, using a culture chamber system, whether direct cell-to-cell interactions between human L$^-$CBMC and FMS/PA6-P cells are also crucial for the expansion of human hematopoietic cells. As shown in Figure 3, the numbers of CD34$^+$cells, CD34$^+$CD38$^-$ cells and CFU-C were significantly lower in non-contact cultures than in contact cultures: L$^-$CBMC in contact cultures showed approximately 98-, 92- and 2.6-fold increases in CD34$^+$ cells, CD34$^+$CD38$^-$ cells and total CFU-C, respectively, whereas L$^-$CBMC in non-contact cultures showed 62-, 58- and 0.72-fold increases in CD34$^+$ cells, CD34$^+$ CD38$^-$ cells and CFU-C, respectively. However, there were no differences in CD34$^+$ cells, CD34$^+$CD38$^-$ cells and CFU-C counts between the non-contact culture and the culture without the FMS/PA6-P cells. These findings suggest that direct cell-to-cell contact between human HSC/progenitor cells and FMS/PA6-P cells is essential for the maximum expansion of human cells, and that the adhesion molecules mediating cell-to-cell contact may be crucial for this maximum expansion.

We have previously shown that FMS/PA6-P cells express a high level of NCAM, and that NCAM contributes greatly to murine hematopoiesis.[20] It can, therefore, be speculated that NCAM may play a crucial role in the human hematopoiesis-supporting capacity of FMS/PA6-P cells. To address this, we examined whether the expansion of the L$^-$CBMC on the FMS/PA6-P cells was inhibited by anti-mouse NCAM monoclonal antibody. The FMS/PA6-P cell layer was pre-incubated with the anti-mouse NCAM monoclonal antibody or an isotype control for 2 h and the L$^-$CBMC were then added to the wells (3.4×10^3 cells/well). The number of L$^-$CBMC adhering to the FMS/PA6-P cell layer was significantly lower (394.0±8.3 cells/well) in the co-cultures to which the anti-

mouse NCAM monoclonal antibody had been added than in the co-cultures to which isotype control had been added (1078.3±315.4 cells/well) (P<0.005) (4 h after inoculation of the L$^-$CBMC on the FMS/PA6-P cells). Two weeks later, the numbers of CD34$^+$ cells, CD34$^+$CD38$^-$ cells and CFU-C were markedly suppressed, in contrast to the numbers in the co-cultures to which isotype control was added (Figure 4). This finding clearly shows that NCAM on the FMS/PA6-P cells plays an important part in supporting human hematopoiesis.

We have found by flow cytometoric analyses that anti-mouse NCAM monoclonal antibody does not react with L$^-$CBMC (*data not shown*), indicating that the monoclonal antibody reacted with murine NCAM expressed on the FMS/PA6-P cells but not with human NCAM expressed on the L$^-$CBMC in the present co-culture system. It is, therefore, conceivable that the monoclonal antibody, which had reacted to mouse NCAM on the FMS/PA6-P cells during the pre-incubation, inhibited the contact between the L$^-$CBMC and NCAM on the FMS/PA6-P cells, and resulted in the low proliferation of the L$^-$CBMC.

Discussion

There is a clear need for *ex vivo* expansion of CB HSC and progenitor cells for successful CB transplantation. However, *in vitro*, it is difficult to enhance the self-renewal and/or expansion of HSC without stromal cells, even if all known exogenous growth factors and other materials are added to the cultures.[23-26] In the present study, we found that mouse mesenchymal stem cells (FMS/PA6-P) show human hematopoiesis-supporting capacity.

When L$^-$CBMC were co-cultured with FMS/PA6-P cells, significantly higher numbers of HSC-enriched population (CD34$^+$CD38$^-$) and progenitor cells (CD34$^+$ cells and CFU-C) were obtained than when they were cultured without FMS/PA6-P cells (Figure 1B). Moreover, significantly higher percentages of human CD45$^+$ cells and CD34$^+$CD38$^-$ cells were detected in the BM of the SCID mice that had received the L$^-$CBMC cultured with FMS/PA6-P cells than in the BM of SCID mice that had received Lin-CBMC cultured without FMS/PA6-P cells (Figure 2A). These findings suggest that FMS/PA6-P cells provide a microenvironment that promotes the proliferation of functional human HSC and progenitor cells. However, we cannot exclude the possibility that some multipotent HSC, which had been contained in the inoculated L$^-$CBMC, were induced to differentiate into their progenitor cells under the influence of exogenous cytokines.

Stromal cells promote the growth, survival and differentiation of HSC and progenitor cells by expressing cell adhesion molecules in addition to producing various growth factors and matrix proteins.[27-30] In the present experiments, we found that there were no differences in CD34$^+$ cells, CD34$^+$CD38$^-$ cells and CFU-C between the non-contact culture of L$^-$CBMC with FMS/PA6-P cells and the culture of L$^-$CBMC without FMS/PA6-P cells (Figure 3). However, in the contact culture, much higher numbers of CD34$^+$ cells, CD34$^+$CD38$^-$ cells and CFU-C counts were obtained. These findings clearly show that direct cell-to-cell contact between L$^-$CBMC and FMS/PA6-P cells is essential for the maximum expansion of the L$^-$CBMC.

We have previously demonstrated that NCAM is highly expressed by FMS/PA6-P cells and contributes greatly to the murine hematopoiesis-supporting capacity of the stromal cells; hematopoiesis was markedly suppressed when anti-mouse NCAM monoclonal antibody was added to the co-culture system of mouse HSC and FMS/PA6-P cells.[21] In the present study, we also observed that the addition of anti-mouse NCAM monoclonal antibody to

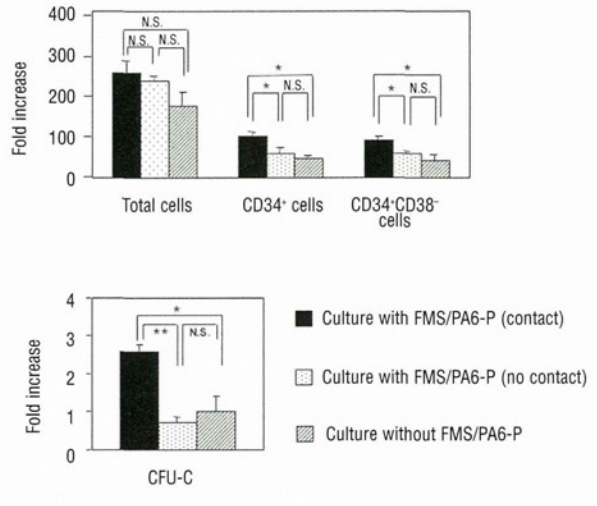

Figure 3. Higher proliferation and differentiation of L$^-$CBMC in contact culture with FMS/PA6-P cells. The monolayer of FMS/PA6-P cells was prepared in a 24-well plate and the L$^-$CBMC were loaded into the culture chamber inserts or directly into the FMS/PA6-P cell monolayer. As a negative control, L$^-$CBMC were cultured without FMS/PA6-P cells. Two weeks later, all cells in the well were collected by trypsin-EDTA treatment, and the fold increases of total cells, CD34$^+$ cells, CD34$^+$CD38$^-$ cells and CFU-C counts were calculated, as mentioned in Figure 1B. Each sample was run in triplicate. Representative data from three independent experiments. **P<0.01; *P<0.05, N.S.: not significant.

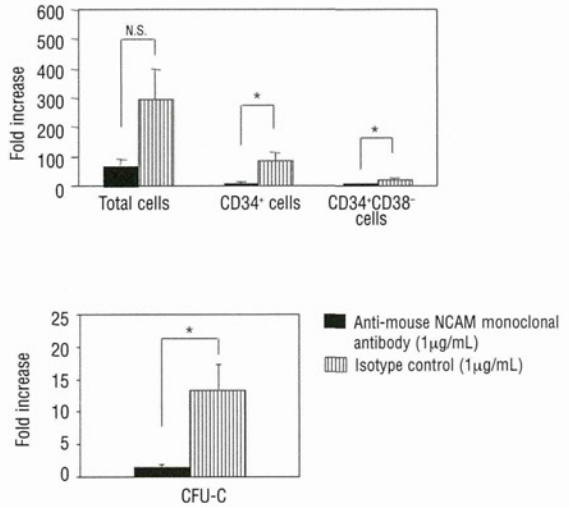

Figure 4. Inhibitory effect of anti-NCAM monoclonal antibody on the proliferation of L$^-$CBMC. The L$^-$CBMC were cultured on the FMS/PA6-P cells in the presence of anti-mouse NCAM monoclonal antibody (5 wells/sample). As a control, the same concentration of isotype control (mouse IgG2a) was added to the culture. Two weeks later, all cells in the well were collected by trypsin-EDTA treatment, and the fold increases of total cells, CD34$^+$ cells, CD34$^+$CD38$^-$ cells and CFU-C counts were calculated, as mentioned in Figure 1B. Mean ± SD of five wells. Representative data from three independent experiments. *P<0.05, N.S.: not significant.

the culture significantly inhibited their contact and the proliferation of L⁻CBMC (Figure 4), suggesting the importance of the NCAM expressed on the FMS/PA6-P cells for human hematopoiesis. The fact that the cDNA sequence of murine NCAM exhibits 94% homology with that of human NCAM[22] may be a reasonable explanation of why murine NCAM on the FMS/PA6-P cells can contribute to human hematopoiesis.

NCAM is known to interact with cell surface molecules by homophilic or heterophilic binding.[31] N-syndecan,[32] heparin sulphate,[33] and fibroblast growth factor-receptor[34] are proposed as ligands of the heterophilic binding. Recently, we found that NCAM is expressed on both a HSC-enriched population (lineage-negative, CD34-positive and blast-gated cells) and BM stromal cells (containing mesenchymal stem cells) in monkeys, and contribute greatly to monkey hematopoiesis.[35] Although the expression of NCAM or its ligand on human HSC has not been well-elucidated, it is possible that NCAM may support human hematopoiesis through homophilic interaction. Our preliminary study showed that commercially-available human mesenchymal stem cells line (#PT-2501, Cambrex Bio Science, Walkersville, MD, USA and #Yub636, Human Science Research Resources Bank, Osaka, Japan) expressed NCAM molecules. The NCAM expression level on these human mesenchymal stem cell lines declined rapidly with the increase of cell passages, whereas there was no decline in other mesenchymal stem cell markers such as CD29, CD73 and CD105. In parallel with the decline in NCAM expression, the cell lines' hematopoiesis-supporting ability was also reduced (*unpublished data*). We observed this phenomenon in the FMS/PA6-P cell line, although the decline in NCAM expression was much more moderate than that of the human mesenchymal stem cell lines.[20] Our further investigation will focus on the molecular mechanisms underlying the interaction between HSC and stromal cells via NCAM in human and mouse hematopoietic systems.

So far, several murine stromal cell lines (e.g. MS-5 cells derived from the BM of adult mouse[15] and embryonic stromal cell lines derived from the aorta-gonad-mesonephros region[36,37]) have been reported to have the ability to support human hematopoiesis. The embryonic stromal cell line expresses Sca-1, VCAM-1 and CD13 [but not PECAM-1, c-kit, CD49d (VLA4α) and CD34] and the VCAM-1/VLA4 pathway has been considered to be one of the most important interactions between HSC/progenitor cells and these stromal cell lines.[37] Although the importance of direct interaction of human HSC and the MS-5 cells was demonstrated by Issaad *et al.*,[15] Nishi *et al.* suggested that cytokines produced by MS-5 cells (granulocyte-colony stimulating factor and stem cell factor) contribute to the human hematopoiesis-supporting activity of the cell line.[38] Here, for the first time, we have shown the importance of NCAM in the interaction between human HSC and the murine stromal cell line.

Multipotent HSC need to interact directly with niche cells in order to maintain their 'stemness'. It has been reported that, in *in vitro* co-culture systems, a higher number of HSC and progenitor cells localize in the stromal cell layer than in the non-adherent cell population.[12,15] Therefore, enzymatic digestion of the adherent cell layer is necessary to collect sufficient numbers of HSC and progenitor cells. However, this treatment is thought to damage these cells. Indeed, we observed decreases in the CFU-C counts after the trypsin-EDTA treatment in the present study. Recently, a unique culture system using temperature-sensitive dishes (RepCell), in which cell detachment is induced by a change in temperature, has been developed. This culture system might be useful for collecting culture-expanded cells from stromal cell layers.

In conclusion, we have shown that the FMS/PA6-P cells can support human hematopoiesis, and that NCAM plays a crucial role in the human hematopoiesis-supporting capacity of these cells. This finding will be of great advantage in improving the clinical application of CB transplantation and other human stem cell transplants. It is also of great importance in further understanding the mechanisms underlying the interaction between human HSC and stromal cells and the regulation of human hematopoiesis.

Authorship and Disclosures

XW and HH contributed to the conception and design of the study, and to the analysis and interpretation of data; XW performed the majority of the experiments and drafted the article; HH revised the article; SI profoundly revised the article and obtained the necessary funding. TM provided the study materials. The other authors contributed to some of the experiments.

The authors reported no potential conflicts of interest.

References

1. Gluckman E. Current status of umbilical cord blood hematopoietic stem cell transplantation. Exp Hematol. 2000;28(11):1197-205.
2. Rubinstein P, Carrier C, Scaradavou A, Kurtzberg J, Adamson J, Migliaccio AR, et al. Outcomes among 562 recipients of placental blood transplants from unrelated donors. N Engl J Med. 1998;339(22):1565-77.
3. Rocha V, Wagner Jr JE, Sobocinski KA, Klein JP, Zhang MJ, Horowitz MM, et al. Graft-versus-host disease in children who have received a cord-blood or bone marrow transplant from an HLA-identical sibling: Eurocord and International Bone Marrow Transplant Registry Working Committeebon Alternative Donor and Stem Cell Sources. N Engl J Med. 2000; 342(25):1846-54.
4. Locatelli F, Rocha V, Chastang C, Arcese W, Michel G, Abecasis M, et al. Factors associated with outcome after cord blood transplantation in children with acute leukemia: Eurocord-Cord Blood Transplant Group. Blood. 1999;93(11):3662-71.
5. Jaroscak J, Goltry K, Smith A, Waters-Pick B, Martin PL, Driscoll TA, et al. Augmentation of umbilical cord blood (UCB) transplantation with ex vivo-expanded UCB cells: results of a phase 1 trial using the AastromReplicell System. Blood. 2003;101(12):5061-7.
6. Stiff P, Chen B, Franklin W, Oldenberg D, His E, Bayer R, et al. Autologous transplantation of ex vivo expanded bone marrow cells grown from small aliquots after high-dose chemotherapy for breast cancer. Blood. 2000;95(6):2169-74.
7. Paquette RL, Dergham ST, Karpf E, Wang HJ, Slamon DJ, Souza L, et al. Ex vivo expanded unselected peripheral blood: progenitor cells reduce posttransplantation neutropenia, thrombocytopenia, and anemia in patients with breast cancer. Blood. 2000;96(7):2385-90.
8. Reichle A, Zaiss M, Rothe G, Schmitz G, Andressen R. Autologous tandem trans-

plantation: almost complete reduction of neutropenic fever following the second transplantation by ex vivo expanded autologous myeloid postprogenitor cells. Bone Marrow Transplant. 2003;32(3):299-305.
9. Mcniece IK, Almeida-Porada G, Shpall EJ, Zanjani E. Ex vivo expanded cord blood cells provide rapid engraftment in fetal sheep but lack long-term engrafting potential. Exp Hematol. 2002;30(6):612-6.
10. Kodama H, Sudo H, Koyama H. Kasai S, Yamamoto S. In vitro hemopoiesis within a microenvironment created by MC 3T3-G2/PA6 preadipocytes. J Cell Physiol. 1984; 118(3):233-40.
11. Dexter TM, Allen TD, Lajtha LG. Conditions controlling the proliferation of hematopoietic stem cells in vitro. J Cell Physiol. 1977;91(3):335-44.
12. Itoh K, Tzuka H, Sakoda H, Konno M, Nagata K, Uchiyama T, et al. Reproducible establishment of hemopoietic supportive stromal cell lines from murine bone marrow. Exp Hematol. 1989:17(2):145-53.
13. Ye ZQ, Burkholder JK, Qiu P, Shahidi NT, Yang NS. et al. Establishment of an adherent cell feeder layer from human umbilical cord blood for support of long-term hematopoietic progenitor cell growth. Proc Natl Acad Sci USA. 1994;91(25):12140-4.
14. Nishikawa M, Ozawa K, Tojo A, Yoshikubo T, Okano A, Tani K, et al. Changes in hematopoiesis-supporting ability of C3H10T1/2 mouse embryo fibroblasts during differentiation. Blood. 1993; 81(5):1184-92.
15. Issaad C, Croisille L, Katz A, Vainchenker W, Coulombel L. A murine stromal cell line allows the proliferation of very primitive human CD34++/CD38- progenitor cells in long-term cultures and semisolid assays. Blood. 1993;81(11):2916-24.
16. Hisha H, Nishino T, Kawamura M, Adachi S, Ikehara S. Successful bone marrow transplantation by bone grafts in chimeric-resistant combination. Exp Hematol. 1995;23(4): 347-52.
17. Ishida T, Inaba M, Hisha H, Sugiura K, Adachi Y, Nagata N, et al. Requirement of donor-derived stromal cells in the bone marrow for successful allogeneic bone marrow transplantation. J Immunol. 1994; 152(6):3119-27.
18. Hashimoto F, Sugiura K, Inoue K, Ikehara S. Major histocompatibility complex restriction between hematopoietic stem cells and stromal cells in vivo. Blood. 1997;89(1):49-54.
19. Sugiura K, Inaba M, Hisha H, Borisov K, Sardina EE, Good RA, et al. Requirement of major histocompatibility complex-compatible microenvironment for spleen colony formation (CFU-S on day 12 but not on day 8). Stem Cells. 1997;15(6):461-8.
20. Wang X, Hisha H, Taketani S, Inaba M, Li Q, Cui W, et al. NCAM contributes to hemopoiesis-supporting capacity of stromal cell lines. Stem Cells. 2005;23(9):1389-99.
21. Wang X, Hisha H, Taketani S, Adachi Y, Li, Q, Cui W, et al. Characterization of mesenchymal stem cells isolated from mouse fetal bone marrow. Stem Cells. 2006;24(3): 482-93.
22. Saito S, Tanio Y, Tachibana I, Hayashi S, Kishimoto T, Kawase I. Complementary DNA sequence encoding the major neural cell adhesion molecule isoform in a human small cell lung cancer cell line. Lung Cancer. 1994;10(5-6):307-18.
23. Bernstein ID, Andrews RG, Zsebo KM. Recombinant human stem cell factor enhances the formation of colonies by CD34+ and CD34+ lin- cells, and the generation of colony-formation cell progeny from CD34+ lin- cells cultured with interleukin-3, granulocyte colony-stimulating factor, or granulocyte-macrophage colony-stimulating factor. Blood. 1991;77(11):2316-21.
24. Lowry PA, Zsebo KM, Deacon DH, Eichman CE, Quesenberry PJ. Effects of rhSCF on multiple cytokine-responsive HPP-CFC generated from Sca-1+ Lin- murine hematopoietic progenitors. Exp Hematol. 1991;19(9):994-6.
25. Li CL, Johnson GR. Stem cell factor enhances the survival but not the self-renewal of murine hematopoietic long-term repopulating cells. Blood. 1994;84(2): 408-14.
26. Ogawa M, Nishikawa S, Ikuta K, Yamamura F, Naito M, Takahashi K, et al. B cell ontogeny in murine embryo studied by a culture system with the monolayer of a stromal cell clone, ST2: B cell progenitor develops first in the embryonal body rather than in the yolk sac. EMBO J. 1988;7(5): 1337-43.
27. Toksoz D, Zsebo KM, Smith KA, Hu S, Brankow D, Suggs SV, et al. Support of human hematopoiesis in long-term bone marrow cultures by murine stromal cells selectively expressing the membrane-bound and secreted forms of the human homologue of the steel gene product, stem cell factor. Proc Natl Acad Sci USA. 1992; 89(16):7350-4.
28. Hannum C, Culpepper J, Campbell D, McClanahan T, Zurawski S, Bazan JF, et al. Ligand for FLT3/FLK2 receptor tyrosine kinase regulates growth of hematopoietic stem cells and is encoded by variant RNAs. Nature. 1994;368(6472):643-8.
29. Satoh M, Mioh H, Shiotsu Y, Ogawa Y, Tamaoki T. Mouse bone marrow stromal cell line MC3T3-G2/PA6 with hematopoietic-supporting activity expresses high levels of stem cell antigen Sca-1. Exp Hematol. 1997;25(9):972-9.
30. Ueno H, Sakita-Ishikawa M, Morikawa Y, Nakano T, Kitamura T, Saito M. A stromal cell-derived membrane protein that supports hematopoietic stem cells. Nature Immunol. 2003;4(5):457-63.
31. Crossin KL, Krushel LA. Cellular signaling by neural cell adhesion molecules of the immunoglobulin superfamily. Dev Dyn. 2000;218(2):260-79.
32. Toba Y, Horie M, Sango K, Tokashiki A, Matsui F, Oohira A, et al. Expression and immunohistochemical localization of heparan sulphate proteoglycan N-syndecan in the migratory pathway from the rat olfactory placode. Eur J Neurosci. 2002; 15(9):1461-73.
33. Gupta P, Oegema TR Jr, Brazil JJ, Dudek AZ, Slungaard A, Verfaillie CM. Structurally specific heparan sulfates support primitive human hematopoiesis by formation of a multimolecular stem cell niche. Blood. 1998;92(12):4641-51.
34. Niethammer P, Delling M, Sytnyk V, Dityatev A, Fukami K, Schachner M. Cosignaling of NCAM via lipid rafts and the FGF receptor is required for neuritogenesis. J Cell Biol. 2002;157(3):521-32.
35. Kato J, Hisha H, Wang X, Mizokami T, Okazaki S, Li Q, et al. Contribution of neural cell adhesion molecule (NCAM) to hemopoietic system in monkeys. Ann Hematol. 2008;87(10):797-807.
36. Xu M, Tsuji K, Ueda T, Mukouyama Y, Hara T, Yang F, et al. Stimulation of mouse and human primitive hemopoiesis by murine embryonic aorta-gonado-mesonephros-derived stromal cell lines. Blood. 1998;92(6):2032-40.
37. Weisel KC, Moore MAS. Genetic and functional characterization of isolated stromal cell lines from the aorta-gonado-mesonephros region. Ann NY Acad Sci. 2005;1044:51-9.
38. Nishi N, Ishikawa R, Inoue H, Nishikawa M, Kakeda M, Yoneya T. Granulocyte-colony stimulating factor and stem cell factor are the crucial factors in long-term culture of human primitive hemopoietic cells supported by a murine stromal cell line. Exp Hematol. 1996;24(11):1312-21.

Journal of Autoimmunity 34 (2010) 380–389

Contents lists available at ScienceDirect

Journal of Autoimmunity

journal homepage: www.elsevier.com/locate/jautimm

The role of dendritic cell subsets in 2,4,6-trinitrobenzene sulfonic acid-induced ileitis☆

Shoichi Hoshino[a,b], Muneo Inaba[a], Hiroshi Iwai[c], Tomoki Ito[d], Ming Li[a], M. Eric Gershwin[e], Kazuichi Okazaki[b], Susumu Ikehara[a,*]

[a] First Department of Pathology, Kansai Medical University, Osaka, Japan
[b] Third Department of Internal Medicine, Kansai Medical University, Osaka, Japan
[c] Department of Otolaryngology, Kansai Medical University, Osaka, Japan
[d] First Department of Internal Medicine, Kansai Medical University, Osaka, Japan
[e] Division of Rheumatology, Allergy-Clinical Immunology, University of California, Davis, USA

ARTICLE INFO

Article history:
Received 19 August 2009
Received in revised form
5 October 2009
Accepted 6 October 2009

Keywords:
Ileitis
Dendritic cells
PIR-A/B
Tolerance

ABSTRACT

Dendritic cells (DCs) are widely distributed throughout the lymphoid and nonlymphoid tissues, and are important initiators of acquired immunity and also serve as regulators by inducing self-tolerance. However, it has not been thoroughly clarified whether DCs are involved in the termination of immune responses. In this paper, we have examined the kinetical movement of dendritic cells (DCs) in the lamina propria using the 2,4,6-trinitrobenzene sulfonic acid (TNBS)-induced ileitis model (an animal model for Crohn's disease). Increased numbers of DCs were recruited to the inflammatory sites from day 1 to day 3 at which time the inflammatory responses was clearly observed, then gradually decreased to a steady-state level on day 7 along with the cessation of responses. Three subsets of DCs, PIR-A/B^{high}, PIR-A/B^{med}, and PIR-A/B^{-} DCs in the CD11c^{+}/B220^{-} conventional DCs (cDCs) were noted on day 3; the number of PIR-A/B^{med} cDCs increased when the inflammatory responses ceased on day 7. The expression of costimulatory molecules such as CD86 and CD54 was lower in the PIR-A/B^{med} DCs compared with the other two cDC subsets or splenic DCs. Furthermore, the stimulatory activity of PIR-A/B^{med} cDCs was lower than those of PIR-A/B^{high} or PIR-A/B^{-} cDCs, and far lower than that of splenic DCs. In addition, an increase in the message level of IL-10 was clearly observed in the PIR-A/B^{med} cDCs on day 7 while that of proinflammatory cytokines such as IL-6 and IL-12 was low. These data demonstrate that PIR-A/B^{med} cDCs which increase at the final stage of inflammation may be involved in the termination of the TNBS-induced ileitis by the delivery of anergic signals to effector T cells due to the lower expressions of costimulatory molecules and the production of immunoregulatory cytokine.

1. Introduction

The use of 2,4,6-trinitrobenzene sulfonic acid (TNBS) is a well known inducer of an animal model of ileitis [1–3]. Although there has been considerable work on this model, the role of mononuclear cell subpopulations and, in particular, the contribution of dendritic cells (DCs), remains unclear. This is particularly important as the model includes both an inductive as well as remitting phase. Indeed, DCs as well as their subsets have been described to modulate, in both a positive and negative fashion, the development of autoimmune responses in multiple other models [4–8].

We have examined these regulatory roles of DCs from the viewpoint of the expression of dual functioning molecule, paired immunoglobulin-like receptors (PIRs). PIR consist of activating (PIR-A) and inhibitory (PIR-B) isoforms, and is known to be expressed on B cells and other myeloid-lineage cells, including

Abbreviations: DCs, dendritic cells; pDCs, plasmacytoid dendritic cells; cDCs, conventional dendritic cells; SI, small intestine; TNBS, 2,4,6-trinitrobenzene sulfonic acid; PIRs, paired immunoglobulin-like receptors; MLR, Mixed leukocyte reaction.

☆ This work was supported by a grant from the Education, Culture, Sports, Science, and Technology; a grant from The 21st Century Center of Excellence (COE) program of the Education, Culture, Sports, Science, and Technology; and also a grant from the Department of Transplantation for Regeneration Therapy (Sponsored by Otsuka Pharmaceutical Co., Ltd.); a grant from Molecular Medical Science Institute, Otsuka Pharmaceutical Co., Ltd.; a grant from Japan Immunoresearch Laboratories Co., Ltd. (JIMRO); and grant from Intractable Diseases, the Health and Labor Sciences Research Grants (KO) from Minister of Labor and Welfare of Japan.

* Corresponding author at: First Department of Pathology, Kansai Medical University, 10-15 Fumizono-cho, Moriguchi City, Osaka 570-8506, Japan. Tel.: +81 6 6993 9429; fax: +81 6 6994 8283.
E-mail address: ikehara@takii.kmu.ac.jp (S. Ikehara).

0896-8411/$ – see front matter © 2009 Elsevier Ltd. All rights reserved.
doi:10.1016/j.jaut.2009.10.002

DCs monocyte/macrophages, neutrophils, eosinophils, mast cells, megakaryocyte/platelets and also on lymphoid progenitor cells committed to differentiation into T cells and NK cells. They are not, however, expressed by mature T cells, NK cells, or erythrocytes [9,10]. PIR-A noncovalently associates with the common γ-chain of Fc receptor bearing ITAM motifs in the cytoplasmic tail that participates in the cell activating signal pathways [11], while PIR-B possesses functional ITIM motifs in their cytoplasmic tails that transduce negative signals in various cellular events [12–15]. It has recently been reported that PIR-B-deficient mice were found to be more susceptible to Salmonella infection than WT mice, and that distinct patterns of postinfectional inflammatory lesions, diffuse spreading along the sinusoids, are found in the liver in PIR-B-deficient mice, while there is nodular restricted localization in WT mice [16]. Furthermore, PIR-B-deficient mice exhibit an exaggerated graft-versus-host (GVH) reaction, possibly due to the interaction between PIR-A on PIR-B$^{-/-}$ DCs and allogeneic MHC class I on donor T cells [17]. These findings clearly show that the imbalance in the expression of PIR-A and PIR-B affects their regulatory roles in host defense, and that the interaction of T cells with DCs through PIRs can also regulate immune responses [18].

In this paper, we have examined the kinetic movement of DCs in the inflammatory sites induced by the injection of 2,4,6-trinitrobenzene sulfonic acid (TNBS). Increased numbers of DCs were recruited to the inflammatory sites on day 3, at which time the inflammatory responses were clearly observed. These responses then gradually decreased to the steady-state level on day 7, beyond which there was a cessation of responses. In the kinetics of DCs, we examined the DC subsets with regard to the expression of PIRs, and found that the number of CD11c^{+} PIR^{low} DCs increased when the inflammatory responses ceased. The APC function of this DC subset was further examined in relation to the expression of costimulatory molecules.

2. Materials and methods

2.1. Animals

Female BALB/c (H-2^{d}) and C57BL/6 (B6, H-2^{b}) mice at the age of 7–10 weeks were purchased from Japan SLC, Inc. (Hamamatsu, Japan). The mice were maintained in our animal facility under specific pathogen-free conditions.

2.2. TNBS-induced gut inflammation

Ileitis was induced by the injection of 2,4,6-trinitrobenzene sulfonic acid (TNBS) (Wako Pure Chemical Industries, Ltd., Osaka, Japan) as described previously [19]. Briefly, the mice underwent a laparotomy under anesthesia. The terminal ileal loop was gently exteriorized on sterile gauze, and 70 μl of 32 mg/ml TNBS solution dissolved in 50% ethanol was then injected transmurally into the lumen 1 cm proximal to the ileocolonic junction. The laparotomy was closed in two layers using non-resorbable nylon sutures. We prepared more than 100 mice, and ileitis was observed in all the mice injected with TNBS. The mice instilled with 50% ethanol alone served as controls ($n = 10$).

2.3. Preparation of small intestine-derived dendritic cells

DCs were isolated as previously described [20]. The small intestine (SI), including the region from the duodenal bulb to the ileocecal junction, was removed, flushed with cold RPMI, and longitudinally opened. The gut was cut into small pieces (~5 mm), and each intestinal segment was transferred to a 50-ml tube containing 25 ml RPMI medium with 1 mM EDTA (Wako Pure Chemical Industries), 1% fetal calf serum (FCS) and 1 mM dithioerythritol (Sigma Aldrich, St. Louis, MO). The tubes were then incubated horizontally at 37 °C for 30 min in a shaking-water bath at 180 rpm. The contents of each tube (intestinal segment and detached cells) were then transferred to Petri dishes and 200 μl FCS added. The intestinal mucosa was gently compressed with a syringe plunger over a nylon mesh, and single-cell suspensions were filtered through nylon mesh and centrifuged for 7 min at 2500 × g. The cell pellets were placed on ice, and 200 μl of FCS and 10 ml of RPMI medium were added and the cell suspensions were filtered through nylon mesh and then centrifuged for 7 min at 2500 × g. The cells were suspended in 4 ml of 40% Percoll® (GE Healthcare UK Ltd, Amersham Place, Little Chalfont, Buckinghamshire HP7 9NA, England) and overlaid onto 4 ml of 70% Percoll. The 40%/70% discontinuous Percoll gradient was centrifuged at 600 × g for 25 min. Cells from the interface were collected, washed and resuspended in RPMI supplemented with 1% FCS. The thus-prepared cells were used as SI-derived DC-enriched cells, and stained with various monoclonal antibodies (mAbs) to characterize their surface immunophenotypes. Dead cells and some epithelial cells were located in a mucous film at the top of the gradient and red blood cells were found in the pellet.

2.4. Surface marker analyses

The cells were stained with fluorescein isothiocyanate (FITC)-conjugated mAb against CD45, CD11c (BD Biosciences, San Jose, CA), Phycoerythrin (PE)-conjugated anti-CD11c, -CD103, PIR-A/B (BD Biosciences), and allophycocyanin (APC)-conjugated anti-CD45R (B220) (CALTAG Laboratories, Invitrogen Corporation, Carlsbad, CA), -CD83 mAbs (eBioscience Inc., San Diego, CA), -CD40, -CD86, and -CD197 mAbs (CCR7), Alexa Fluor 647-conjugated anti-CD54 mAbs, and PE/Cy7-conjugated anti-CD86 mAbs (BioLegend, San Diego, CA) were also used to stain the SI-derived DC-enriched cells. All samples were preincubated with anti-CD16/CD32 mAb to block the nonspecific binding of mAbs through Fc receptors (FC Block, BD Biosciences, San Jose, CA). The cells were analyzed using a FACS Calibur HG (Becton Dickinson and Company, Mountain View, CA). Dead cells were excluded from analysis using propidium iodide staining.

2.5. Isolation of SI-derived dendritic cells

SI-derived DCs were stained with FITC-anti-CD11c, PE-anti-PIR-A/B, and APC-anti-CD45R mAbs, and the cells with the PIR^{high}, PIR^{med}, and PIR$^{low/-}$ immunophenotypes in the CD11c^{+} DCs were separately sorted by a FACSAria (Becton Dickinson and Company).

2.6. Preparation of splenic dendritic cells

Spleen cells were prepared after the injection of collagenase type IV (100 u/ml, SIGMA ALDRICH Japan, Tokyo, Japan) into the spleen, and the spleen cells were overlaid onto 4 ml of 50% Percoll. The Percoll gradient was centrifuged at 600 × g for 25 min, and the cells from the interface were collected, washed and resuspended in PBS supplemented with 2% FCS. The thus-prepared cells were stained with PE-anti-CD11c mAb and FITC-anti-CD3 mAb (BD Biosciences). The stained cells were applied to an EPICS ALTRA® (BECKMAN COULTER Japan, Tokyo, Japan), and CD11c^{+}CD3^{-} cells were isolated as splenic DCs.

2.7. Mixed leukocyte reaction (MLR)

Mixed leukocyte reaction (MLR) was performed to examine the stimulatory activities of SI-derived DC subsets. MLR was performed

as follows: $CD4^+$ T cells were prepared from allogeneic C57BL/6 spleen cells by a "$CD4^+$ T cell isolation kit" (Miltenyi Biotec GmbH). The responder splenic $CD4^+$ T cells (2×10^5) were cultured with graded doses of irradiated (12 Gy) stimulator DCs (SI-derived DCs or splenic DCs) for 72 h and pulsed with 0.5 μCi of [^{3}H]-thymidine for the last 16 h of the culturing period. Splenic DCs were used as positive control APCs.

2.8. Histopathological analysis

The tissue specimens were fixed in buffered formalin and embedded in paraffin, and the sections were stained with hematoxylin and eosin.

2.9. Immunohistochemical analyses

The intestinal tissue was embedded in a compound (Tissue-Tek®, Sakura Finetechnics Co., Ltd., Tokyo, Japan) and frozen in acetone. The cryostat sections at 6 μm in thickness were stained with FITC-conjugated anti-CD45R and PE-conjugated anti-CD11c mAbs (diluted in Tris-buffered saline containing 1% bovine serum albumin). Cellular nuclei were counterstained with DAPI (NACALAI TESQUE Inc., Kyoto, Japan). The stained samples were analyzed using a confocal laser microscope (LSM 510 META; Carl Zeiss IMT Corporation, Oberkochen, Germany).

2.10. Real-time RT-PCR assay

Cytokine messages of SI-derived DC subsets were determined by real-time RT-PCR. Total RNA of each sample was quantified using an ND-1000 spectrophotometer (NanoDrop Technologies, Inc., Wilmington, DE). The quality of the RNA was verified by an Agilent 2100 bio-analyzer (Agilent Technologies, Palo Alto, CA). Real-time PCR was performed in an ABI PRISM 7900HT machine (Applied Biosystems) using SYBR Green PCR Master Mix (Applied Biosystems), according to the manufacturer's instructions in a total volume of 25 μl. Cycling conditions for IL-6, IL-10, and IL-12 genes were 2 min at 50 °C, 10 min at 94 °C, 45 cycles of 15 s at 94 °C, 30 s at 60 °C, 1 min at 72 °C. To correlate the threshold (Ct) values from the amplification plots to copy number, a standard curve was generated, and a non-template control was run with every assay.

We prepared two pairs of primers for
Mouse IL-6:
5′-ACAACCACGGCCTTCCCTAC-3′ (sense),
5′-ACAATCAGAATTGCCATTGCAC-3′ (antisense)
Mouse IL-10:
5′-CCAAGCCTTATCGGAAATGA-3′ (sense),
5′-TCTCACCCAGGGAATTCAAA-3′ (antisense)
Mouse IL-12:
5′-GGTTTGCCATCGTTTTGC TG-3′ (sense),
5′-GAGGTTCACTGTTTCTCC AG-3′ (antisense)

2.11. Detection of cytokines in the culture supernatant

Culture supernatants of SI-derived DC subsets were collected 24 h later, and the amount of IL-6, IL-10, IL-12p70, TNF-α, IFN-γ, and MCP-1 were determined by BD™ Cytometric Bead Array, Mouse Inflammation Kit (BD Biosciences). The data were analyzed using FCAP Array Software (BD Biosciences).

2.12. Statistical analysis and ethical considerations

Differences between groups were examined for statistical significance using the Mann–Whitney test. A P value less than 0.05 was considered statistically significant. The experimental protocol and all experiments were approved by the Animal Experimentation Committee, Kansai Medical University.

3. Results

3.1. Histological examination of TNBS-induced ileitis

We first kinetically analyzed the course of inflammation by histological examination. From 1 to 3 days after the injection of TNBS, the destruction of villi structure, the infiltration of inflammatory cells such as granulocytes, macrophages, and small numbers of lymphocytes gradually increased (Fig. 1A and B), and on day 5, the thickening of the submucosal layer and muscle layer was clearly observed (Fig. 1C). However, these inflammatory changes healed, and normal histological findings appeared by day 7. None of the control mice injected with 50% ethanol alone showed any histopathological change in the small intestine throughout the duration of the experiment (from day 1 to day 7).

3.2. Kinetic of DCs in the inflammatory site

Along with the exacerbation of TNBS-induced ileitis, the frequency of $CD11c^+$ DCs increased from day 1 to day 3, then gradually decreased to the steady-state level on day 7, at which time the ileitis had resolved (Fig. 2). $CD11c^+$ DCs are positive for CD103, indicating that the DCs we observed are of lamina propria origin. As also shown in Fig. 2B, though there was an obvious increase in the number of $CD11c^+/B220^-$ conventional DCs (cDCs), the frequency of $CD11c^+/B220^+$ plasmacytoid DCs (pDCs) remained unchanged. This is the case when the TNBS-induced ileitis was cytohistochemically examined. In the steady state, small numbers of cDCs were observed in the lamina propria and, along with the progress of ileitis, the number increased in this area and then gradually decreased (data not shown). These findings suggest that the kinetics of cDCs, but not pDCs, was associated with the initiation and termination of TNBS-induced ileitis.

3.3. Immunophenotype of DCs on the expression of PIR

We next determined the expression of PIR-A/B on SI-derived DCs in the kinetics of TNBS-induced ileitis. As shown in Fig. 3A, we observed two main populations, as to the expression of PIR-A/B in SI-derived cDCs ($CD11c^+/B220^-$) in the steady state (on day 0, before the injection of TNBS), PIR-A/B^- and PIR-A/B^{high} cDCs. Then, on day 3 SI-derived cDCs were clearly separated into 3 cDC populations (PIR-A/B^{high}, PIR-A/B^{med}, and PIR-A/B^-); the PIR-A/B^{med} cDC subset was clearly detected on day 3 and thereafter. The kinetic changes in these populations along with the progress of the TNBS-induced ileitis were examined and are summarized in Fig. 3B. Note that the frequency of PIR-A/B^- cDCs gradually increased on day 3 and then drastically decreased under the steady-state level, while that of PIR-A/B^{med} cDCs appeared on day 3 and then drastically increased from day 5 to day 7, at which time the TNBS-induced ileitis terminated. The number of PIR-A/B^{high} cDCs remained largely unchanged, though a slight increase was observed on day 5. Since the frequency of total cDCs reduced to the normal level (Fig. 2), only PIR-A/B^{med} cDCs increased along with the termination of the inflammatory responses. This profile of the expression of PIR-A/B was only observed in the DCs of lamina propria origin. Splenic DCs (or the Peyer's patch DCs) did not show this profile in which only DCs with the PIR-A/B^{high} phenotype were clearly observed (Fig. 3C and D).

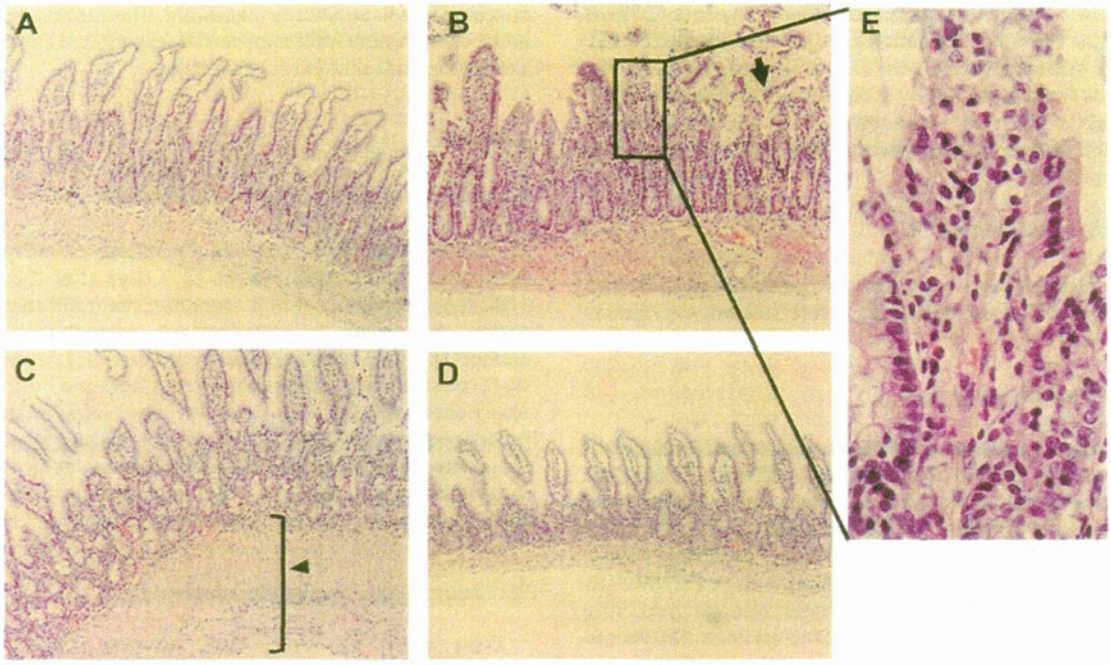

Fig. 1. Histological examination of the TNBS-induced ileitis. The tissue specimens were removed on day 1 (A), day 3 (B, E), day 5 (C), and day 7 (D) after the injection of TNBS, and were fixed, embedded in paraffin, and the sections then stained with hematoxylin and eosin. From 1 to 3 days after the injection of TNBS, the destruction of villi structure (B, arrow), the infiltration of inflammatory cells such as granulocytes, macrophages, and small numbers of lymphocytes gradually increased (B and E, enlargement of the square of B), and on day 5, the thickening of submucosal and muscle layers was clearly observed (C, arrow head). These inflammatory changes healed, and normal histological findings appeared by day 7. The results are representative of 5 replicate experiments. (A–D: magnification 200×, E: magnification 400×.)

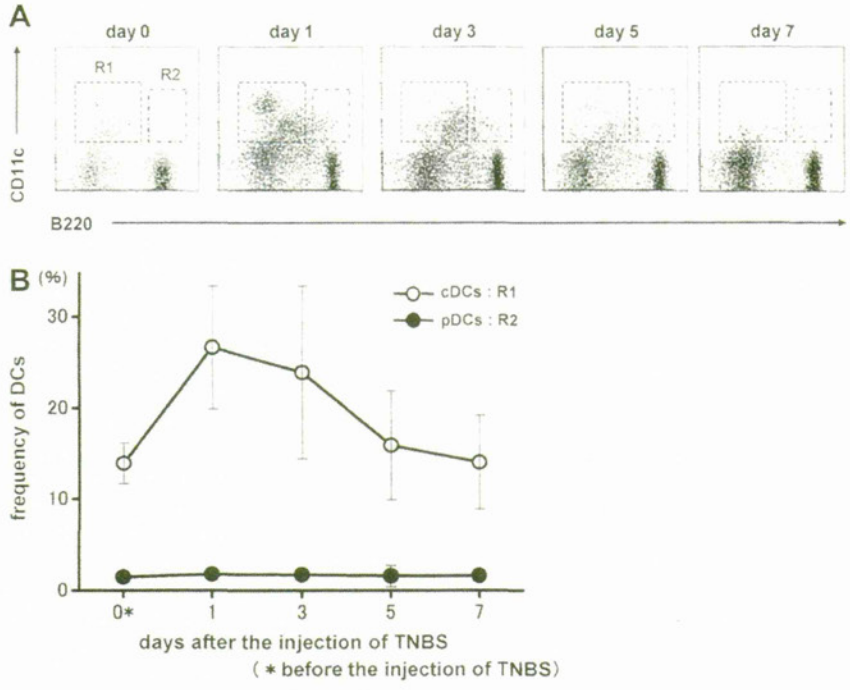

Fig. 2. Kinetics of DCs in the lamina propria in the TNBS-induced ileitis. A DC-enriched population was prepared from the small intestine on days 1, 3, 5, and 7 after the injection of TNBS and stained with FITC-anti-CD45, PE-anti-CD11c, and APC-anti-B220 (CD45R) mAbs to determine the kinetics of cDCs and pDCs. $CD45^+$ cells were defined as hemopoietic-lineage cells, and in $CD45^-$ cells, cDCs were defined as $CD11c^+/B220^-$ cells (R1 in dot plot profiles), and pDCs were defined as $CD11c^+/B220^+$ cells (R2 in dot plot profiles) (A). Kinetics of cDCs (open circles) and pDCs (closed circles) are shown in Fig. 1B. Symbols and bars in the figure represent the mean ± SDs of 5 mice, and the results are representative of 2 replicate experiments. Dead cells were gated out by the staining of cells with propidium iodide.

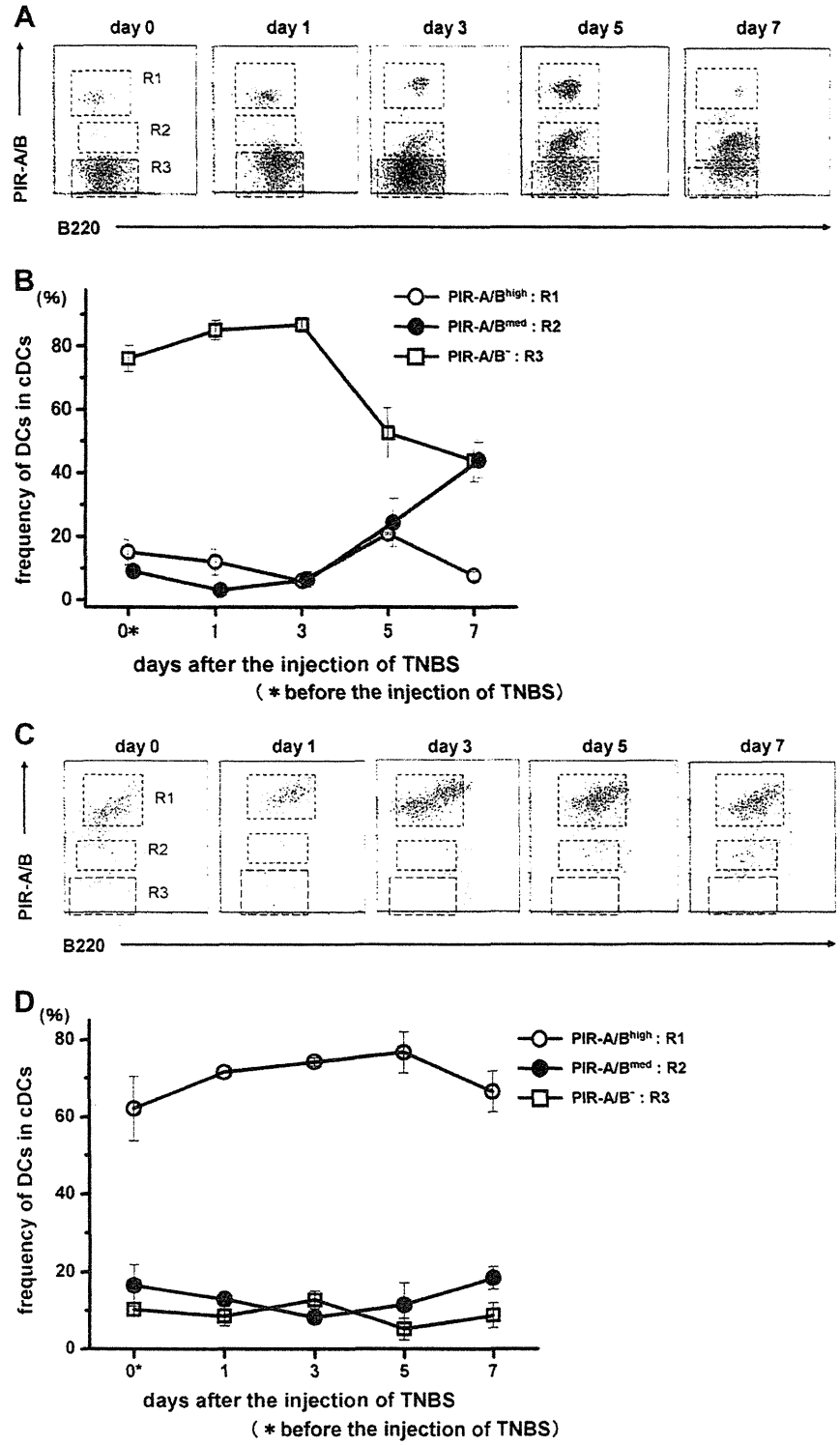

Fig. 3. Expression of PIR-A/B on DCs. (A) A DC-enriched population was prepared from the small intestine on days 1, 3, 5, and 7 after the injection of TNBS and stained with FITC-anti-CD11c, PE-anti-PIR-A/B, and APC-anti-CD45R mAbs. SI-derived cDCs (gated as $CD11c^{+}/B220^{-}$ cells) were separated into 3 populations on the basis of the expression of PIR-A/B, $PIR\text{-}A/B^{high}$, $PIR\text{-}A/B^{med}$, and $PIR\text{-}A/B^{-}$ cDCs (on days 3–7). The results are representative of 5 replicate experiments. (B) Kinetics of DC subsets based on the expression of PIR-A/B, $PIR\text{-}A/B^{high}$ (open circles), $PIR\text{-}A/B^{med}$ (closed circles), and $PIR\text{-}A/B^{-}$ (open squares) cDCs are summarized. Symbols and bars in the figure represent the mean ± SDs of 5 mice, and the results are representative of 2 replicate experiments. (C) Splenocytes were prepared on days 1, 3, 5, and 7 after the injection of TNBS and stained with FITC-anti-CD11c, PE-anti-PIR-A/B, and APC-anti-B220 mAbs. The splenic cDCs were defined as $CD11c^{+}/B220^{-}$ cells. Though splenic cDCs were separated into 3 populations on the basis of the expression of PIR-A/B, only those with the $PIR\text{-}A/B^{high}$ phenotype were clearly observed (R1 in C, and D). The results are representative of 5 replicate experiments. (D) Kinetics of splenic DC subsets based on the expression of PIR-A/B, $PIR\text{-}A/B^{high}$ (open circles), $PIR\text{-}A/B^{med}$ (closed circles), and $PIR\text{-}A/B^{-}$ (open squares) cDCs are summarized. Symbols and bars in the figure represent the mean ± SDs of 5 mice, and the results are representative of 2 replicate experiments.

3.4. Expression of costimulatory molecules on PIR-A/B^{med} cDCs

If the PIR-A/B^{med} cDCs that specifically increased when the TNBS-induced ileitis terminated are somehow involved in the termination process of immune responses, the regulatory features of this population should be compared with those of the PIR-A/B^{high} or PIR-A/B^{-} cDCs. Therefore, we determined that the costimulatory molecules (such as CD86 and CD54) are important elements in the immunological synapse, helping to deliver the second signal to activate T cells. As shown in Fig. 4A, the expression of CD86 was clearly low in the PIR-A/B^{med} cDCs compared with PIR-A/B^{high} cDCs throughout the inflammatory process, and that of CD54 on the PIR-A/B^{med} cDCs was also lower than that expressed on PIR-A/B^{high} cDCs or PIR-A/B^{-} cDCs. Note that the expression of CD86 and CD54 on splenic DCs with the PIR-A/B^{high} phenotype (main population of splenic DCs) was high, comparable to or higher than those expressed on SI-derived PIR-A/B^{high} or PIR-A/B^{-} cDCs. The expression of CD40, CD83 and CCR7 remained unchanged throughout the inflammatory processes in these subsets (data not shown).

3.5. Stimulatory activity of PIR-A/B^{med} cDCs

The stimulatory activities of SI-derived DC subsets, PIR-A/B^{high}, PIR-A/B^{med} or PIR-A/B^{-} cDCs, were determined by MLR. As shown in Fig. 5B, the stimulatory activity of PIR-A/B^{med} cDCs obtained on day 7 was lower than those of PIR-A/B^{high}, and far lower than that of splenic DCs used as positive control DCs, suggesting that the number of PIR-A/B^{med} cDCs increased during the final stage of inflammation, and that they might be involved in terminating the TNBS-induced ileitis by the delivery of anergic signals due to the lower expression of costimulatory molecules, as shown in Fig. 4. Furthermore, it is noted that though the frequency of PIR-A/B^{high} cDCs on day 1 was not so high (Fig. 3), the stimulatory activity of PIR-A/B^{high} cDCs was high and comparable to that of splenic DCs when the inflammatory response had started (Fig. 5A, day 1). This is in accordance with the expression of costimulatory molecules (CD86 and CD54) on this subset of DCs. Therefore, these findings show that the immune responses were probably initiated by the PIR-A/B^{high} cDCs on day 1, and attenuated or reduced by the

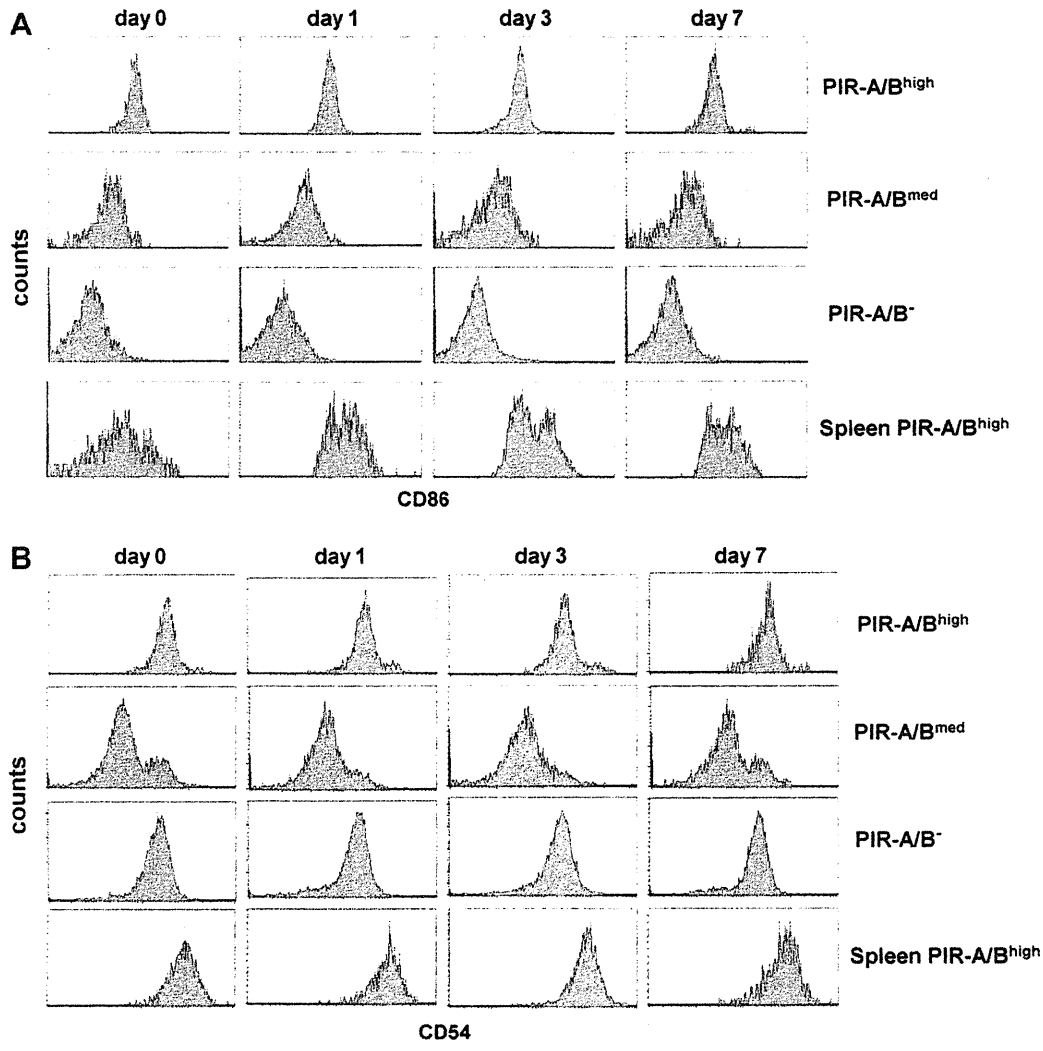

Fig. 4. Expression of costimulatory molecules on PIR-A/B^{med} cDCs. A DC-enriched population was prepared from the small intestine on days 1 and 7 after the injection of TNBS and stained with FITC-anti-CD11c, PE-anti-PIR-A/B, APC-anti-B220 or PE-Cy7-anti-B220, and APC-anti-CD86 or PE-Cy7-anti-CD54 mAbs. The expression of CD86 (A) or CD54 (B) on the PIR-A/B^{med} cDCs (CD11c^{+}/B220^{-} cells) was compared with that on the PIR-A/B^{high} or PIR-A/B^{-} cDCs. Splenic cDCs (CD11c^{+}/B220^{-} cells) with the PIR-A/B^{high} phenotype were used as a positive control. The results are representative of 3 replicate experiments.

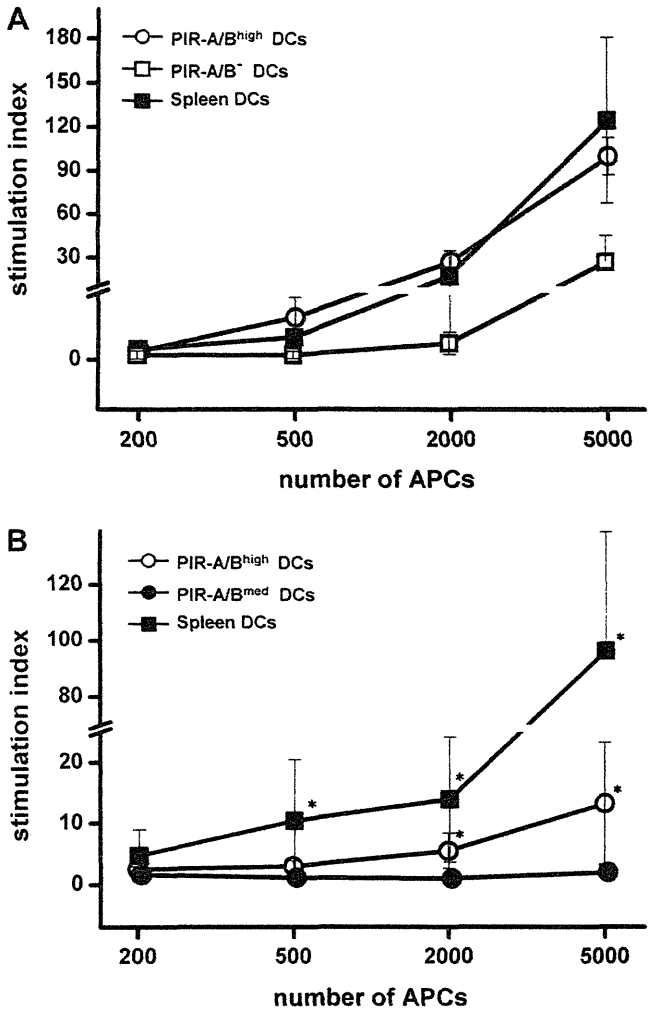

Fig. 5. Stimulatory activity of PIR-A/B^{med} cDCs. A DC-enriched population was prepared from the small intestine on day 7 after the injection of TNBS, and PIR-A/B^{high} (open circles), PIR-A/B^{med} (closed circles), and PIR-A/B$^-$ (open squares) cDCs were sorted after the staining with FITC-anti-CD11c, PE-anti-PIR-A/B, and APC-anti-B220 mAbs. Splenic cDCs prepared as CD11c$^+$/B220$^-$ DCs were used as positive control DCs (closed squares). The responder splenic CD4$^+$ T cells (2×10^5) from C57BL/6 mice were cultured with graded doses of various stimulator DCs for 72 h and pulsed with 0.5 μCi of [^{3}H]-thymidine for the last 16 h of the culturing period. Symbols and bars in the figure represent the mean ± SDs of 5 mice, and the results are representative of 2 replicate experiments. "A" shows the stimulatory activity of SI-derived cDC subsets purified from the mice 1 day after the injection of TNBS, and "B" shows that purified from the mice 7 days after the injection of TNBS. *$P < 0.05$.

PIR-A/B^{med} cDCs that appeared on days 3–7 with lower expression of costimulatory molecules.

3.6. Cytokine production in PIR-A/B^{med} cDCs

To determine the characteristic feature of the PIR-A/B^{med} cDCs in the cytokine production, a real-time RT-PCR assay was carried out. As shown in Fig. 6, the message level of IL-10 having the immunoregulatory function was clearly augmented in the PIR-A/B^{med} cDCs on day 7 (Fig. 6A) when compared with that in PIR-A/B^{high} cDCs (on day 1, Fig. 6C and day 7, Fig. 6B), while proinflammatory cytokines such as IL-6 and IL-12 were down-regulated in the PIR-A/B^{med} cDCs (Fig. 6A). In contrast, the PIR-A/B$^-$ cDCs, which gradually increased on day 3 and then drastically decreased (Fig. 3B), expressed high IL-12 message on day 1 (though IL-10 message was also high), and the PIR-A/B^{high} cDCs with low frequency on day 1 (Fig. 3B) but high stimulatory activity (Fig. 5A) had elevated IL-6 message (Fig. 6C). Thus the PIR-A/B$^-$ cDCs and the PIR-A/B^{high} cDCs produce proinflammatory or immunopotentiating cytokines at the beginning of the inflammatory response (on day 1). This was confirmed when the amounts of IL-6, IL-10, and IL-12p70 in the culture supernatants of PIR-A/B^{med} cDCs were determined using a Cytometric Bead Array (data not shown).

4. Discussion

It is recognized that dendritic cells (DCs), which are distributed throughout the lymphoid and nonlymphoid tissues, are important initiators of acquired immunity by stimulating naïve T cells and also serve as regulators by inducing self-tolerance [21]. In the case of the invasion of pathogenic microorganisms, immature DCs in the periphery sense these microbes as "danger signals" by pattern recognition receptor such as TLRs, and then serve as migratory cells in the afferent lymph, and finally as APCs in the regional lymph nodes. Furthermore, in the steady-state condition, peripheral DCs reach lymph nodes and contribute to maintaining peripheral tolerance in the absence of strong maturation signals. Thus, DCs control the immune responses from a number of different aspects. However, inflammatory responses evoked by the invasion of microbes usually cease within 7–10 days, and the mechanism(s) leading to the termination of immune responses might be complex. Possible mechanisms employed to terminate inflammation include TGF-β from macrophages, anti-inflammatory lipoxins and the inhibition of proinflammatory cytokines.

Inflammatory responses generally initiate acquired immune responses because pathogens to evoke inflammatory responses or inflammatory responses themselves are recognized by sentinel DCs as "danger signals". Thus the termination of inflammatory responses should be linked to the cessation of immune responses. The de-activation of T cells or the activation of regulatory T cells such as Tr-1, Th3 or Treg, or the recently-reported myeloid-derived suppressor cells that suppress T cell responses, could also participate in this process [22–25]. De-activation of T cells is attributable to apoptosis as a final stage of the activation process, or the induction of the anergic state by the signal delivered via CTLA-4, which is usually expressed after the activation of T cells [26,27]. Recently, there is mounting evidence that the termination of immune responses is also controlled by DCs, where antigen-specific Treg can be activated to suppress effector T cells after the interaction with antigen-presenting DCs [28]. Furthermore, tolerogenic/regulatory DCs are induced in the particular cytokine milieu consisting of GM-CSF, IL-10, and TGF-β [29], terminating the acute lethal systemic inflammatory responses. This type of DCs are not only induced but are naturally present *in vivo* as a subset of DCs with the immunophenotype of CD11c^{low}CD45RB^{high} [30]. Thus, DCs can control the initiation and termination of immune responses.

The expression of various cell surface molecules and the production of certain cytokines are important mechanisms by which DCs are able to regulate immune responses. In this paper, we have first focused on the functional differences of SI-derived DCs in respect to the expression of PIR molecules. We have analyzed the kinetics of DCs in the region of ileitis induced by the injection of TNBS transmurally into the lumen of the small intestine. TNBS-induced ileitis developed and was typically observed at 3 days when histologically examined, and spontaneously resolved at 7 days. The kinetics of the SI-derived cDCs or pDCs is depicted in Fig. 1, which shows that there is a strong correlation between the accumulation of these DCs and the inflammatory response. However, when DCs are characterized as to the expression of PIR-A/B, a distinctive pattern of recruitment is observed. PIR-AB is expressed on DCs, and

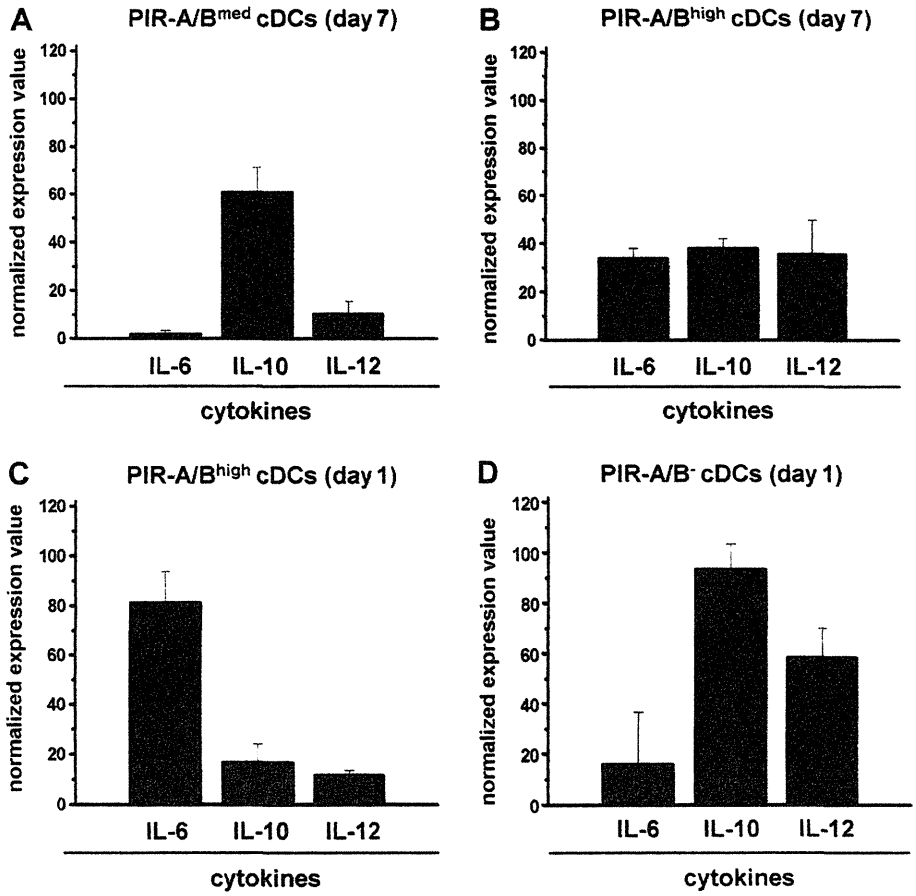

Fig. 6. Production of immunoregulatory cytokine in PIR-A/B^{med} cDCs. Cytokine messages of SI-derived DC subsets were determined by real-time RT-PCR. Purified cDC subset, the PIR-A/B^{med} cDCs (A), PIR-A/B^{high} cDCs (B and C), or PIR-A/B^{-} cDCs (D) were prepared from the ileitis-induced mouse on day 1 or day 7. After DNase I treatment, cDNA was synthesized, amplified using IL-6, IL-10 or IL-12 primer, and visualized with SYBR Green by real-time RT-PCR. Relative intensity of cytokine mRNA was calculated on the basis of GAPDH intensity. Columns represent relative cytokine message levels of IL-6, IL-10 and IL-12. Each column shows mean ± SD of 3 mice and we performed two separate experiments.

has been reported to regulate immune responses [16,17]. In SI-derived DCs, almost all the cDCs are positive for CD103, indicating that these are lamina propria cDCs. When stained with mAb against PIR-A/B, three cDC subsets (PIR-A/B^{high}, PIR-A/B^{med} and PIR-A/B^{-}) were clearly observed, and on a note of caution, PIR-A/B^{med} cDCs were detected on day 3 and only this subset increased at 7 days, at which point the inflammatory responses terminated. No histopathological changes were observed in the small intestine of the control mice injected with 50% ethanol alone, and no PIR-A/B^{med} cDCs were detected throughout the duration of the experiment. This subset of SI-derived DCs show lower expression of CD86 and CD54, the former being essential to deliver the second signal to T cells, and the latter being involved in the formation of the immunological synapse. Furthermore, it is of importance that the stimulatory activity of PIR-A/B^{med} cDCs is lower than that of PIR-A/B^{high}, PIR-A/B^{-} or splenic DCs. Therefore, it is feasible that this subset of DCs is involved in terminating the immune responses (driven by TNBS) to induce the anergic state to effector T cells. In pDCs, it has been reported that CCR9-expressing pDCs suppress immune responses (acute graft-versus-host disease) in the gut [31].

Recently it has been reported that intestinal DCs display specialized functions, including the ability to promote gut tropism to lymphocytes, to polarize noninflammatory responses, and to drive the differentiation of adaptive Foxp3^{+} Treg cells. It is of interest that intestinal epithelial cells drive the differentiation of Treg-promoting DCs, which counteracts Th1 and Th17 development [32]. In our studies, the development of or increase in Treg has not been observed in accordance with the frequency of PIR-A/B^{med} cDCs (data not shown), indicating that PIR-A/B^{med} cDCs with low expression of costimulatory molecules directly induce the anergic state in effector T cells. Furthermore, EC-derived TGF-β and/or retinoic acid might contribute to the functional modulation of DCs where DCs upregulated CD103 and acquired a tolerogenic phenotype [33]. However, the expression of CD103 on PIR-A/B^{high}, PIR-A/B^{med}, PIR-A/B^{-} cDCs subsets of DCs remained unchanged, again indicating that the induction of the anergic state to effector T cells by PIR-A/B^{med} cDCs is a possible mechanism for terminating the immune response, and that this might be due to the insufficient expression of costimulatory molecules on this subset. The effect of tolerogenic or regulatory DCs has been confirmed by systemic administration of these DCs to an inflammatory arthritis model of mice, where TNF-α-treated DCs were able to bias T cell responses towards an anti-inflammatory profile and were shown to ameliorate collagen-induced arthritis. Thus, in agreement with our study, TNF-α-treated DCs can reduce the proinflammatory response and direct the immune system towards the anti-inflammatory state [34]. Furthermore, IL-10-treated human dendritic cells induce Th2 cell allergen tolerance by driving the differentiation of regulatory T cells [35]. One of the mechanisms by which the immune response is terminated is the production of tryptophan degradates such as kynurein, which is produced by DCs after the activation of indoleamine-pyrrole 2,3-dioxygenase (IDO) [36]. We should emphasize

that these data further highlight the role of immune regulation in modulating the evolution of an immune response. This is clearly influenced by both the adaptive response and also the genetics/epigenetics of the host; this is well exemplified in multiple other models of autoimmunity and inflammation [37–42].

This is the first report that SI-derived cDCs can be divided into three subsets on the basis of the expression of PIR-A/B, and that PIR-A/B^{med} cDCs might be involved in the termination of immune responses. Though the precise mechanism(s) underlying this phenomenon is still unclear, the delivery of anergic signals (Fig. 5) due to the lower expression of costimulatory molecules on PIR-A/B^{med} cDCs (Fig. 4) is one of the feasible machineries to terminate the immune responses by this cDC subset. Furthermore, the message level of IL-10 having the immunoregulatory function was clearly augmented in PIR-A/B^{med} cDCs on day 7 (Fig. 6A) while those of proinflammatory cytokines such as IL-6 and IL-12 were low when compared with PIR-A/B^{high} cDCs and PIR-A/B^{-} cDCs (on day 1, Fig. 6C and D). In these DCs, proinflammatory cytokines were clearly detected. Therefore, PIR-A/B^{med} cDCs with lower expression of costimulatory molecules can also participate in the termination of immune responses by the production of immunoregulatory cytokines such as IL-10. We are now further investigating whether the regulatory cytokine milieu (such as IL-10) is actually involved in the increase in PIR-A/B^{med} cDCs. Furthermore, recent research indicates that the production of indoleamine 2,3-dioxygenase (IDO) by DCs inhibits T cell proliferation through tryptophan degradation [43,44]. Therefore, the increase in the activity of IDO in PIR-A/B^{med} cDCs is a possible mechanism for the de-activation of effector T cells and the termination of inflammatory responses. The activity of IDO in the SI-derived DC subsets should be compared (using the IDO inhibitor 1-methyl-dl-tryptophan), and appropriate experiments are now underway. In addition, to further elucidate the role of PIR-A/B^{med} cDCs, the following experiments are now in progress: i) the adoptive cell transfer of PIR-A/B^{med} cDCs into a colitis-induced murine model to examine whether PIR-A/B^{med} cDCs ameliorate the TNBS-induced colitis and facilitate recovery, ii) the use of PIR-A-, PIR-B- [16,17] or DC-deficient mice to assess the development of disease, and iii) the analyses of some signaling pathways downstream of the PIR-A or -B tail, since it has recently been reported that protein tyrosine phosphatases (SHP-1 and SHP-2) are required for PIR-B-mediated inhibitory signaling [13]. The correlation of SI-derived subsets on the expression of PIR-A/B should be further examined to determine whether the up- or down-regulation of PIR-A/B on these subsets takes place, resulting in the conversion of the immunophenotype.

Recent reports have indicated that myeloid-derived suppressor cells (MDSCs) co-expressing Gr-1 and CD11b inhibit T cell activation in various tumor-bearing models [45,46]. Moreover the cells characterized as MDSCs, which lacked stimulatory activity to allogeneic T cells and suppressed T cell proliferation, were also detected in patients with hepatocellular carcinoma [47]. Furthermore, of importance is that MDSCs were detected not only in the model mouse of inflammatory bowel disease (IBD) but also observed in the peripheral blood from patients with IBD [48]. It has been reported that the numbers of human MDSCs, identified as CD14^{+}/HLA-DR$^{-/low}$ cells, increase in both patients with active ulcerative colitis and those with Crohn's disease. The generation of MDSCs in these IBDs indicates that regulatory mechanisms may be initiated by the inflammatory state that terminate the inflammatory or immune responses. In our model system, PIR-A/B^{med} cDCs were induced during the inflammatory state, and probably served as the regulatory cells (such as MDSCs) in other animal models and in clinical findings. Therefore, the possibility that MDSCs are also induced in our model system should be examined along with the analyses of the kinetics of PIR-A/B^{med} cDCs. Furthermore, these findings suggest the possible therapeutic usage of such immunoregulatory PIR-A/B^{med} cDCs or MDSCs for patients with active chronic IBDs.

We have found that PIR-A/B^{med} cDCs drastically increased along with the termination of the TNBS-induced ileitis. This newly discovered DC subset in the small intestine might be involved in the termination of immune responses by the delivery of anergic signals to effector T cells due to the lower expression of costimulatory molecules and the production of immunoregulatory cytokine.

Author contribution

Contribution: S.H. performed the majority of the experiments and analyzed data; M.I. designed and performed the experiments, analyzed data, and prepared the manuscript; H.I., T.I., M.L., M.E.G., and K.O. analyzed the data and contributed to manuscript writing; and S.I. coordinated experiments and prepared the manuscript.

Conflict-of interest disclosure: The authors declare no competing financial interests.

Acknowledgments

The authors thank Ms. K. Ando and Mr. Hilary Eastwick-Field for their help in the preparation of the manuscript, and also thank Mr. Hiroyuki Gonda, Central Research of Laboratory, for his help in the flowcytometrical analyses.

References

[1] Tsujikawa T, Ohta N, Nakamura T, Satoh J, Uda K, Ihara T, et al. Medium-chain triglycerides modulate ileitis induced by trinitrobenzene sulfonic acid. J Gastroenterol Hepatol 1999;14:1166–72.
[2] Goldhill JM, Stojadinovic A, Kiang J, Smallridge R, Shea-Donohue T. Hyperthermia prevents functional, histological and biochemical abnormalities induced during ileitis. Neurogastroenterol Motil 1999;11:69–76.
[3] Moreels TG, De Man JG, Dick JM, Nieuwendijk RJ, De Winter BY, Lefebvre RA, et al. Effect of TNBS-induced morphological changes on pharmacological contractility of the rat ileum. Eur J Pharmacol 2001;423:211–22.
[4] Abraham M, Karni A, Dembinsky A, Miller A, Gandhi R, Anderson D, et al. In vitro induction of regulatory T cells by anti-CD3 antibody in humans. J Autoimmun 2008;30:21–8.
[5] Gonnella PA, Waldner H, Del Nido PJ, McGowan FX. Inhibition of experimental autoimmune myocarditis: peripheral deletion of TcR Vbeta 8.1, 8.2+ CD4^{-} T cells in TLR-4 deficient mice. J Autoimmun 2008;31:180–7.
[6] Lleo A, Selmi C, Invernizzi P, Podda M, Gershwin ME. The consequences of apoptosis in autoimmunity. J Autoimmun 2008;31:257–62.
[7] Venkatesh J, Kawabata D, Kim S, Xu X, Chinnasamy P, Paul E, et al. Selective regulation of autoreactive B cells by FcgammaRIIB. J Autoimmun 2009;32:149–57.
[8] Xiao X, Ma B, Dong B, Zhao P, Tai N, Chen L, et al. Cellular and humoral immune responses in the early stages of diabetic nephropathy in NOD mice. J Autoimmun 2009;32:85–93.
[9] Kubagawa H, Burrows PD, Cooper MD. A novel pair of immunoglobulin-like receptors expressed by B cells and myeloid cells. Proc Natl Acad Sci U S A 1997;94:5261–6.
[10] Kubagawa H, Chen CC, Ho LH, Shimada TS, Gartland L, Mashburn C, et al. Biochemical nature and cellular distribution of the paired immunoglobulin-like receptors, PIR-A and PIR-B. J Exp Med 1999;189:309–18.
[11] Maeda A, Kurosaki M, Kurosaki T. Paired immunoglobulin-like receptor (PIR)-A is involved in activating mast cells through its association with Fc receptor gamma chain. J Exp Med 1998;188:991–5.
[12] Blery M, Kubagawa H, Chen CC, Vely F, Cooper MD, Vivier E. The paired Ig-like receptor PIR-B is an inhibitory receptor that recruits the protein-tyrosine phosphatase SHP-1. Proc Natl Acad Sci U S A 1998;95:2446–51.
[13] Maeda A, Kurosaki M, Ono M, Takai T, Kurosaki T. Requirement of SH2-containing protein tyrosine phosphatases SHP-1 and SHP-2 for paired immunoglobulin-like receptor B (PIR-B)-mediated inhibitory signal. J Exp Med 1998;187:1355–60.
[14] Maeda A, Scharenberg AM, Tsukada S, Bolen JB, Kinet JP, Kurosaki T. Paired immunoglobulin-like receptor B (PIR-B) inhibits BCR-induced activation of Syk and Btk by SHP-1. Oncogene 1999;18:2291–7.
[15] Uehara T, Blery M, Kang DW, Chen CC, Ho LH, Gartland GL, et al. Inhibition of IgE-mediated mast cell activation by the paired Ig-like receptor PIR-B. J Clin Invest 2001;108:1041–50.

[16] Torii I, Oka S, Hotomi M, Benjamin Jr WH, Takai T, Kearney JF, et al. PIR-B-deficient mice are susceptible to *Salmonella* infection. J Immunol 2008;181:4229–39.
[17] Nakamura A, Kobayashi E, Takai T. Exacerbated graft-versus-host disease in $Pirb^{-/-}$ mice. Nat Immunol 2004;5:623–9.
[18] Takai T. A novel recognition system for MHC class I molecules constituted by PIR. Adv Immunol 2005;88:161–92.
[19] Kolgazi M, Jahovic N, Yuksel M, Ercan F, Alican I. Alpha-lipoic acid modulates gut inflammation induced by trinitrobenzene sulfonic acid in rats. J Gastroenterol Hepatol 2007;22:1859–65.
[20] Resendiz-Albor AA, Esquivel R, Lopez-Revilla R, Verdin L, Moreno-Fierros L. Striking phenotypic and functional differences in lamina propria lymphocytes from the large and small intestine of mice. Life Sci 2005;76:2783–803.
[21] Steinman RM, Nussenzweig MC. Avoiding horror autotoxicus: the importance of dendritic cells in peripheral T cell tolerance. Proc Natl Acad Sci U S A 2002;99:351–8.
[22] Gabrilovich DI, Nagaraj S. Myeloid-derived suppressor cells as regulators of the immune system. Nat Rev Immunol 2009;9:162–74.
[23] Roncarolo MG, Gregori S, Battaglia M, Bacchetta R, Fleischhauer K, Levings MK. Interleukin-10-secreting type 1 regulatory T cells in rodents and humans. Immunol Rev 2006;212:28–50.
[24] Sakaguchi S, Yamaguchi T, Nomura T, Ono M. Regulatory T cells and immune tolerance. Cell 2008;133:775–87.
[25] Veldman C, Nagel A, Hertl M. Type I regulatory T cells in autoimmunity and inflammatory diseases. Int Arch Allergy Immunol 2006;140:174–83.
[26] Scalapino KJ, Daikh DI. CTLA-4: a key regulatory point in the control of autoimmune disease. Immunol Rev 2008;223:143–55.
[27] Rudd CE. CTLA-4 co-receptor impacts on the function of Treg and $CD8^-$ T-cell subsets. Eur J Immunol 2009;39:687–90.
[28] Mellow AL, Munn DH. IDO expression by dendritic cells: Tolerance and tryptophan catabolism. Nat Rev Immunol 2004;4:762–74.
[29] Sato K, Yamashita N, Yamashita N, Baba M, Matsuyama T. Regulatory dendritic cells protect mice from murine acute graft-versus-host disease and leukemia relapse. Immunity 2003;18:367–79.
[30] Fujita S, Seino K, Sato K, Sato Y, Eizumi K, Yamashita N, et al. Regulatory dendritic cells act as regulators of acute lethal systemic inflammatory response. Blood 2006;107:3656–64.
[31] Hadeiba H, Sato T, Habtezion A, Oderup C, Pan J, Butcher EC. CCR9 expression defines tolerogenic plasmacytoid dendritic cells able to suppress acute graft-versus-host disease. Nat Immunol 2008;9:1253–60.
[32] Iliev ID, Mileti E, Matteoli G, Chieppa M, Rescigno M. Intestinal epithelial cells promote colitis-protective regulatory T-cell differentiation through dendritic cell conditioning. Mucosal Immunol 2009;2:340–50.
[33] Coombes JL, Siddiqui KR, Arancibia-Carcamo CV, Hall J, Sun CM, Belkaid Y, et al. A functionally specialized population of mucosal $CD103^+$ DCs induces $Foxp3^+$ regulatory T cells via a TGF-beta and retinoic acid-dependent mechanism. J Exp Med 2007;204:1757–64.
[34] Healy LJ, Collins HL, Thompson SJ. Systemic administration of tolerogenic dendritic cells ameliorates murine inflammatory arthritis. Open Rheumatol J 2008;2:71–80.
[35] Li X, Yang A, Huang H, Zhang X, Town J, Davis B, et al. Induction of Th2 cell allergen tolerance by IL-10-differentiated regulatory dendritic cells. Am J Respir Cell Mol Biol 2009.
[36] Grohmann U, Orabona C, Fallarino F, Vacca C, Calcinaro F, Falorni A, et al. CTLA-4-Ig regulates tryptophan catabolism in vivo. Nat Immunol 2002;11:1097–101.
[37] Harrison LC, Honeyman MC, Morahan G, Wentworth JM, Elkassaby S, Colman PG, et al. Type 1 diabetes: lessons for other autoimmune diseases? J Autoimmun 2008;31:306–10.
[38] Hewagama A, Richardson B. The genetics and epigenetics of autoimmune diseases. J Autoimmun 2009;33:3–11.
[39] Jordan MA, Baxter AG. The genetics of immunoregulatory T cells. J Autoimmun 2008;31:237–44.
[40] Kessel A, Bamberger E, Masalha M, Toubi E. The role of T regulatory cells in human sepsis. J Autoimmun 2009;32:211–5.
[41] Morahan G, Peeva V, Mehta M, Williams R. Systems genetics can provide new insights in to immune regulation and autoimmunity. J Autoimmun 2008;31:233–6.
[42] Morris GP, Brown NK, Kong YC. Naturally-existing CD4(+)CD25(+)Foxp3(+) regulatory T cells are required for tolerance to experimental autoimmune thyroiditis induced by either exogenous or endogenous autoantigen. J Autoimmun 2009;33:68–76.
[43] Terness P, Bauer TM, Röse L, Dufter C, Watzlik A, Simon H, et al. Inhibition of allogeneic T cell proliferation by indoleamine 2,3-dioxygenase-expressing dendritic cells: mediation of suppression by tryptophan metabolites. J Exp Med 2002;196:447–57.
[44] Hwu P, Du MX, Lapointe R, Do M, Taylor MW, Young HA. Indoleamine 2,3-dioxygenase production by human dendritic cells results in the inhibition of T cell proliferation. J Immunol 2000;164:3596–9.
[45] Bunt SK, Sinha P, Clements VK, Leips J, Ostrand-Rosenberg S. Inflammation induces myeloid-derived suppressor cells that facilitate tumor progression. J Immunol 2006;176:284–90.
[46] Song X, Krelin Y, Dvorkin T, Bjorkdahl O, Segal S, Dinarello CA, et al. $CD11b^+$/$Gr\text{-}1^+$ immature myeloid cells mediate suppression of T cells in mice bearing tumors of IL-1-secreting cells. J Immunol 2005;175:8200–8.
[47] Hoechst B, Ormandy LA, Ballmaier M, Lehner F, Kruger C, Mann MP, et al. A new population of myeloid-derived suppressor cells in hepatocellular carcinoma patients induces $CD4^+CD25^+Foxp3^+$ T cells. Gastroenterology 2008;135:234–43.
[48] Haile LA, von Wasielewski R, Gamrekelashvili J, Kruger C, Bachmann O, Westendorf AM, et al. Myeloid-derived suppressor cells in inflammatory bowel diseases: a new immunoregulatory pathway. Gastroenterology 2008;136:871–81.

Int J Hematol
DOI 10.1007/s12185-011-0820-0

ORIGINAL ARTICLE

Clinical significance of subcategory and severity of chronic graft-versus-host disease evaluated by National Institutes of Health consensus criteria

Takayuki Sato · Tatsuo Ichinohe · Junya Kanda · Kouhei Yamashita · Tadakazu Kondo · Takayuki Ishikawa · Takashi Uchiyama · Akifumi Takaori-Kondo

Received: 12 October 2010 / Revised: 21 February 2011 / Accepted: 16 March 2011

Abstract To evaluate the clinical significance of subcategory and severity of chronic graft-versus-host disease (GVHD) as defined by the National Institutes of Health (NIH) consensus criteria, we retrospectively studied 211 patients with hematologic neoplasms who survived beyond 100 days after allogeneic hematopoietic cell transplantation. Endpoints included chronic GVHD-specific survival (cGSS), duration of immunosuppressive treatment, and non-relapse mortality (NRM). A total of 96 patients fulfilled the NIH diagnostic criteria for cGVHD. In univariable analysis, patients with NIH overlap syndrome tended to exhibit lower cGSS compared to those with NIH classic cGVHD [hazard ratio (HR) = 2.76, $P = 0.060$], while patients with severe cGVHD at onset had a significantly lower cGSS compared to those with mild-to-moderate cGVHD (HR = 3.10, $P = 0.034$). The duration of immunosuppressive treatment was not significantly affected by either subcategory or severity of NIH cGVHD. In multivariable analysis treating cGVHD as a time-dependent covariate, development of overlap syndrome (HR = 3.90, $P = 0.014$) or severe cGVHD at peak worsening (HR = 6.21, $P < 0.001$) was significantly associated with higher risk of NRM compared to the absence of cGVHD. Our results suggest that both the subcategory and severity of NIH cGVHD are partly correlated with cGSS and may play a useful role in distinguishing patients at high risk for NRM, warranting validation of this approach through future prospective studies.

Keywords Hematopoietic cell transplantation · Chronic graft-versus-host disease · NIH consensus criteria

1 Introduction

Chronic graft-versus-host disease (cGVHD) remains a serious complication associated with substantial late morbidity and mortality after allogeneic hematopoietic cell transplantation (allo-HCT). In contrast to acute GVHD (aGVHD), which preferentially affects specific organs such as the skin, liver, and gastrointestinal tract, cGVHD presents with protean organ dysfunctions and various degrees of immunodeficiency that is further worsened by immunosuppressive medications used for relieving symptoms associated with GVHD [1]. Previous studies have identified a variety of factors that increase the risk of the development of cGVHD, including a prior history of aGVHD, older patient age, use of alloimmune female donors for male recipients, transplants from unrelated or human leukocyte antigen (HLA)-mismatched donors, and use of peripheral blood grafts [2–10]. In this context, clinical management of cGVHD has increasingly become more important, because recent trends in allo-HCT such as expanding applications of peripheral blood stem cell

A part of this study was presented as an abstract at the 51th Annual Meeting of American Society of Hematology, New Orleans, LA, USA, December 6, 2009.

T. Uchiyama: Deceased.

T. Sato · T. Ichinohe (✉) · J. Kanda · K. Yamashita · T. Kondo · T. Ishikawa · T. Uchiyama · A. Takaori-Kondo
Department of Hematology and Oncology,
Graduate School of Medicine, Kyoto University,
54 Shogoin Kawaharacho, Sakyo-ku, Kyoto 606-8507, Japan
e-mail: nohe@kuhp.kyoto-u.ac.jp

Present Address:
J. Kanda
Division of Cellular Therapy,
Duke University Medical Center, Durham, NC, USA

Published online: 05 April 2011

transplantation after reduced-intensity conditioning in older patients may increase the incidence of cGVHD [11].

Historically, aGVHD and cGVHD were distinguished based on whether immune-mediated organ dysfunction occurred within 100 days or more than 100 days after transplantation. However, accumulating experience has indicated that clinical manifestations similar to aGVHD can develop even several months after allo-HCT, while GVHD with typical features of the "chronic" form can occur as early as 2 months post-transplantation [12, 13]. Therefore, an arbitrary classification using the timing of GVHD onset is no longer considered appropriate. Another drawback in the management of cGVHD is that the grading criteria for its severity has not been standardized: it is difficult to predict the risk of GVHD-associated mortality by using historic classification that categorizes cGVHD into limited and extensive subtypes [14], because clinical severity as well as organ involvement of patients classified as having extensive cGVHD varies considerably [15–17].

To resolve these issues, the National Institutes of Health (NIH) consensus criteria were recently proposed to standardize the diagnosis and global assessment of cGVHD with a new severity scoring system based on organ-specific manifestations taking functional impact into account [18]. The NIH criteria distinguished two subcategories of cGVHD, "classic cGVHD" without features of aGVHD and "an overlap syndrome" in which characteristic features of both cGVHD and aGVHD are simultaneously present. In particular, features of aGVHD occurring beyond day 100 without manifestations of classic cGVHD are classified as "persistent", "recurrent", or "late-onset" aGVHD. Based on the number of involved organs and the severity within affected organs, each subcategory of cGVHD was graded into mild, moderate, or severe subtype. However, clinical significance of NIH cGVHD subcategory as well as their severity is not fully established, although several studies have shown their impact on overall survival, cGVHD-specific survival (cGSS), and non-relapse mortality (NRM) [19–23].

In the present study, we retrospectively evaluated patients who received allo-HCT for intractable hematologic disorders with special focus on the influences of subcategory and severity of NIH cGVHD on clinical outcomes. Since probabilities of GVHD-specific survival and discontinued immunosuppressive treatment (IST) have been most commonly used as surrogate endpoints representing the clinical resolution of cGVHD [24–26], we analyzed factors associated with these outcomes in patients who developed NIH cGVHD. We also evaluated the impact of the presence or absence of each subtype of NIH cGVHD on NRM.

2 Patients and methods

2.1 Patients

We retrospectively reviewed the medical records of 259 consecutive patients with hematologic disorders who underwent allo-HCT between January 2000 and December 2008 in our department and survived at least 100 days after transplantation. Patients were excluded if they had a history of previous allo-HCT ($n = 24$), rejected graft ($n = 4$), or relapsed before day 100 ($n = 20$); thus, a total of 211 patients were included in the present analysis. No patients received donor lymphocyte infusions before day 100. Patients with malignant hematologic neoplasms were defined as having standard-risk disease if they underwent transplantation in first complete remission or without prior chemotherapy, while those who underwent transplantation in any other status were classified as having high-risk disease. Patients with aplastic anemia were considered to have standard-risk disease. This study was approved by the Ethics Committee of Kyoto University Graduate School of Medicine. Written informed consent for the transplantation protocol was obtained from all patients.

2.2 Transplantation procedure

Patients with malignant hematologic neoplasms received myeloablative or fludarabine-based reduced-intensity conditioning regimens with or without total-body irradiation (TBI) as described elsewhere [27, 28]. Patients with aplastic anemia received conditioning regimens consisting of high-dose cyclophosphamide and horse or rabbit anti-lymphocyte globulin with or without 2–4 Gy TBI. None of these patients received T-cell-depleted grafts. All patients received GVHD prophylaxis by the use of cyclosporine or tacrolimus combined with or without short-term methotrexate. A proportion of patients given transplants from HLA-mismatched family members or unrelated marrow donors received mycophenolate mofetil in addition to tacrolimus plus methotrexate as GVHD prophylaxis [28]. All patients received supportive care including blood product transfusion and prophylaxis against opportunistic infections according to our institutional protocols [29].

2.3 Evaluation and management of acute and chronic GVHD

All patients were graded for aGVHD using conventional criteria, and the maximum grade until day 100 after transplantation was assigned [30]. Patients who developed grade II–IV aGVHD were initially treated with methylprednisolone or prednisolone usually at a dose of 1–2 mg/kg. Treatment of steroid-refractory aGVHD was variable.

The incidence of cGVHD was retrospectively evaluated by using the NIH consensus criteria [18]. Patients who had at least one "diagnostic" clinical sign or at least one "distinctive" manifestation, confirmed by relevant laboratory tests or histologic examination, were defined as having cGVHD if other possible diagnoses were excluded. Subclassification of cGVHD into "classic cGVHD" and "overlap syndrome" was strictly according to the NIH criteria. If patients had any features of aGVHD along with classic cGVHD, they were classified as having an overlap syndrome. The severity of cGVHD was assessed at its onset and at maximal clinical worsening and graded into "mild", "moderate", and "severe" categories according to the global scoring system defined by the NIH criteria. Treatment of cGVHD was variable, but followed some general principles; patients with isolated mouth, ocular, or localized skin cGVHD were treated only with topical therapy, while patients with more symptomatic cGVHD were treated with systemic immunosuppressive agents such as prednisolone at a dose of 0.5–1.0 mg/kg per day combined with calcineurin inhibitors. Although the duration and dosing of those agents were not standardized, patients typically received treatment until all symptoms of cGVHD were resolved or stabilized. Patients with less severe symptoms were often treated with peroral low-dose prednisolone at a dose of less than 0.5 mg/kg per day.

2.4 Statistical analysis

Descriptive statistics were used to summarize variables related to patient and transplant characteristics. Comparisons among the groups were performed by use of extended Fisher exact test for categorical variables and Wilcoxon–Mann–Whitney test for continuous variables. The primary endpoint of the study was cGSS, which is defined as the time from the day of diagnosis of cGVHD to the day of death in the absence of relapse or secondary malignancy, among patients who developed NIH cGVHD stratified by its subcategory or severity at onset. The probabilities of cGSS were estimated according to the Kaplan–Meier method, and univariable comparison between groups was made using the log-rank test. Patients who were alive without recurrent or secondary malignancy were censored at their last follow-up visit and those who experienced recurrent or secondary malignancy were censored at the time of its diagnosis. The time to discontinuation of IST was defined among patients who received systemic IST for the treatment of NIH cGVHD as the time from the day of diagnosis of cGVHD to the day of withdrawal of systemic IST. NRM was defined among all patients included in the study as rates of death without evidence of primary disease recurrence. The incidence rates of IST withdrawal and those of NRM were estimated with the use of the cumulative incidence method to accommodate the following competing events [31]: the onset of recurrent or secondary malignancy and death from any cause for IST withdrawal, and the recurrent primary disease for NRM. Cox proportional-hazards regression models were used to evaluate variables potentially associated with cGSS, while competing risks regression models were used to evaluate variables potentially associated with IST withdrawal and NRM [32]. The variables included in the analysis were as follows: patient age, donor–recipient sex combination, disease status at the time of transplantation, donor–recipient HLA compatibility, stem cell sources, type of conditioning regimens, grades of prior aGVHD (grades 0–1 vs. grades 2–4), subcategory of NIH cGVHD (classic cGVHD vs. overlap syndrome), global severity of NIH cGVHD at onset (mild to moderate vs. severe), platelet counts, eosinophil counts, and administration of systemic corticosteroids at the onset of cGVHD. In the analysis to evaluate the impact of the presence of each NIH cGVHD subtype on NRM for the entire cohort of patients in the study, development of each subtype of cGVHD was treated as a time-dependent covariate under the assumption that a patient who developed moderate or severe cGVHD could not revert to less severe cGVHD and that classic cGVHD and overlap syndrome could not switch to each other [33]. Factors having two-sided P values less than 0.1 for association with outcome were included in multivariable model using a forward and backward stepwise method with a predetermined risk of 0.1. Two-sided P values <0.05 were considered to be statistically significant. All analyses were performed using STATA version 11 (College Station, TX, USA) according to patient information available as of 1 July 2009.

3 Results

3.1 Patient characteristics

Table 1 shows the characteristics of the 211 patients included in the study; they had a median age of 46 years, included 113 males and 98 females, and underwent transplantation for malignant hematologic neoplasms in most cases. The number of patients who received bone marrow, peripheral blood, and cord blood unit was 152 (72%), 44 (21%), and 15 (7%), respectively. After a median follow-up of 37.2 months (range 3.3–111.6), a total of 96 patients (45%) developed manifestations of cGVHD that met the NIH consensus criteria. There was no statistically significant difference in background characteristics between patients who developed NIH cGVHD and those who did not, except that the former group included higher proportion of patients with a history of antecedent grade II–IV aGVHD.

Table 1 Patient and transplantation characteristics

Characteristic	All patients ($n = 211$)	NIH cGVHD		
		Absent ($n = 115$)	Present ($n = 96$)	P value
Median patient age, years (range)	46 (17–69)	46 (19–69)	47 (17–67)	0.90
Donor/recipient sex combination, n (%)				0.17
Male/male	66 (31)	41 (35)	25 (26)	
Male/female	42 (20)	21 (18)	21 (22)	
Female/female	56 (27)	33 (29)	23 (24)	
Female/male	47 (22)	20 (17)	27 (28)	
Diagnosis, n (%)				0.59
Myeloid neoplasms	113 (54)	65 (57)	48 (50)	
Precursor lymphoid neoplasms	31 (15)	17 (15)	14 (15)	
Mature lymphoid neoplasms	61 (29)	29 (25)	32 (33)	
Aplastic anemia	6 (3)	4 (3)	2 (2)	
Disease status at transplant, n (%)				0.41
Standard risk	105 (50)	54 (47)	51 (53)	
High risk	106 (50)	61 (53)	45 (47)	
Donor type[a], n (%)				0.71
HLA-matched related	83 (39)	45 (39)	38 (40)	
HLA-mismatched related	23 (11)	12 (10)	11 (11)	
HLA-matched unrelated	89 (42)	47 (41)	42 (44)	
HLA-mismatched unrelated	16 (8)	11 (10)	5 (5)	
Donor/recipient HLA compatibility[a], n (%)				0.59
Matched	172 (82)	92 (80)	80 (83)	
Mismatched	39 (18)	23 (20)	16 (17)	
Stem cell source, n (%)				0.30
Bone marrow	152 (72)	85 (74)	67 (70)	
Peripheral blood	44 (21)	20 (17)	24 (25)	
Cord blood	15 (7)	10 (9)	5 (5)	
Conditioning regimen, n (%)				0.55
Myeloablative with TBI	113 (54)	64 (56)	49 (51)	
Myeloablative without TBI	15 (7)	10 (9)	5 (5)	
Reduced intensity with TBI	65 (31)	33 (29)	32 (33)	
Reduced intensity without TBI	18 (9)	8 (7)	10 (10)	
GVHD prophylaxis, n (%)				0.73
Tacrolimus based	169 (80)	91 (79)	78 (81)	
Cyclosporine based	42 (20)	24 (21)	18 (19)	
Prior aGVHD, n (%)				0.048
Grade 0–1	117 (55)	70 (61)	47 (49)	
Grade 2	72 (34)	38 (33)	34 (35)	
Grade 3–4	22 (10)	7 (6)	15 (16)	
Median months (range) after transplantation[b]	37.2 (3.3–111.6)	35.6 (3.3–111.6)	40.6 (4.0–105.3)	0.14

cGVHD chronic graft-versus-host disease, *aGVHD* acute graft-versus-host disease, *TBI* total-body irradiation

[a] HLA matching was defined by 2-digit compatibility at HLA-A, -B, and -DRB1 loci

[b] Median follow-up months among patients who were alive at the time of last follow-up

Table 2 summarizes the characteristics of 96 patients who developed NIH cGVHD according to its subcategory; 77 (80%) developed "classic cGVHD" and 19 (20%) developed "overlap syndrome". A total of 31 (40%) patients with classic GVHD and 18 (95%) with overlap syndrome had a prior history of grade II–IV aGVHD. The

median time from transplantation to the onset of cGVHD in patients with overlap syndrome was shorter compared to patients with classic cGVHD (4.1 vs. 7.1 months, $P < 0.001$). All patients with overlap syndrome were graded as having moderate or severe cGVHD, whereas the proportion of patients who developed severe cGVHD was similar between patients with classic cGVHD and those with overlap syndrome. Proportions of patients with platelet counts less than $100 \times 10^3/\mu L$, eosinophil counts less than 500/μL, and ongoing systemic corticosteroid treatment at the onset of cGVHD were higher among patients who developed overlap syndrome compared with those who developed classic cGVHD.

3.2 Chronic GVHD-specific survival

Of the 96 patients who developed NIH cGVHD, recurrent or secondary malignant neoplasm occurred in 27 patients and death due to any cause occurred in 31 patients. The respective 3-year probabilities of cGSS among patients who developed classic cGVHD and overlap syndrome were 88 and 70% ($P = 0.060$) (Fig. 1a), while those among subgroups of patients graded to have mild, moderate, and severe cGVHD at onset were 100, 86, and 69% (mild to moderate vs. severe, $P = 0.034$) (Fig. 1b). Table 3 shows the results of univariable and multivariable analyses for factors potentially associated with cGSS among the patients who developed NIH cGVHD. In univariable analysis, the presence of severe cGVHD and thrombocytopenia at cGVHD onset were significantly associated with lower cGSS, whereas the presence of an overlap syndrome and high-risk malignant disease tended to be associated with lower cGSS. In multivariable analysis, the presence of thrombocytopenia at cGVHD onset was the only significant factor that adversely affected cGSS [hazard ratio (HR) for mortality = 4.05, 95% confidence interval (CI) = 1.35–12.1, $P = 0.013$], although patients with severe cGVHD (HR = 2.58, 95% CI = 0.90–7.39, $P = 0.077$) or those with high-risk underlying disease (HR = 2.75, 95% CI = 0.86–8.80, $P = 0.088$) also had a trend toward lower cGSS.

3.3 Duration of systemic immunosuppressive treatment

A total of 81 patients received systemic immunosuppressive agents for the treatment of NIH cGVHD. In this group of patients, the cumulative incidence of withdrawal of systemic IST was 40% (95% CI = 29–51%) at 3 years after the onset of cGVHD, while the cumulative incidence of the competing risks of death or recurrent/secondary malignancy during systemic IST was 42% (95% CI = 32–55%) (Fig. 2). In univariable analysis, no significant association was found between discontinuation of IST and subcategory or global severity of NIH cGVHD (overlap syndrome vs. classic cGVHD, HR for IST withdrawal = 0.51, 95% CI = 0.20–1.31, $P = 0.16$; severe vs. mild to moderate, HR = 0.90, 95% CI = 0.42–1.96, $P = 0.80$). Multivariable analysis revealed two factors significantly associated with prolonged administration of systemic IST; high-risk primary disease (HR = 0.39, 95% CI = 0.19–0.77, $P = 0.007$) and the ongoing use of systemic corticosteroids at the onset of cGVHD (HR = 0.40, 95% CI = 0.19–0.84, $P = 0.015$).

3.4 Non-relapse mortality

Death from non-relapse causes occurred in 16 (17%) of 96 patients who developed NIH cGVHD and in 10 (9%) of 115 patients who did not. In a multivariable analysis of the entire series of 211 patients, treating the subcategory or peak severity of NIH cGVHD as a time-dependent covariate, development of the overlap syndrome or severe cGVHD was significantly associated with higher risk of NRM compared to the absence of cGVHD (overlap syndrome vs. no cGVHD, HR = 3.90, 95% CI = 1.32–11.6, $P = 0.014$; severe cGVHD vs. no cGVHD, HR = 6.21, 95% CI = 2.25–17.1, $P < 0.001$). Development of classic cGVHD or mild-to-moderate cGVHD was not significantly associated with higher risk of NRM when compared with the absence of NIH cGVHD (classic cGVHD vs. no cGVHD, HR for mortality = 1.39, 95% CI = 0.55–3.53, $P = 0.49$; mild-to-moderate cGVHD vs. no cGVHD, HR = 2.25, 95% CI = 0.62–8.18, $P = 0.22$).

4 Discussion

In the present study, we evaluated the clinical significance of subcategory and severity of NIH cGVHD in terms of their influences on cGSS, discontinuation of IST, and NRM using a retrospective cohort of patients who underwent allo-HCT for hematologic disorders. In univariable analysis, patients with overlap syndrome tended to have a lower probability of cGSS than those with classic cGVHD, while patients who developed severe cGVHD had significantly worse cGSS compared with those who developed mild-to-moderate cGVHD. Although such differences in cGSS according to NIH cGVHD subtypes did not reach statistical significance by multivariable analysis, patients who developed overlap syndrome or severe NIH cGVHD had a significantly higher NRM than those who did not develop any manifestation of NIH cGVHD. These results suggest that both subcategory and global severity of NIH cGVHD might be useful for evaluating the risk of GVHD-associated mortality in patients diagnosed to have cGVHD by the NIH criteria. In

Table 2 Characteristics of chronic GVHD according to subcategory defined by the National Institutes of Health criteria

Characteristics	Total ($n = 96$)	NIH cGVHD subcategory		
		Classic cGVHD ($n = 77$)	Overlap syndrome ($n = 19$)	P value
Median months (range) to onset of cGVHD	6.7 (2.1–29.9)	7.1 (2.7–29.9)	4.1 (2.1–20.7)	<0.001
Involved organs or sites[a], n (%)[b]				0.92
Skin	55 (57)	40 (52)	15 (79)	
Mouth	69 (72)	56 (73)	13 (68)	
Eyes	29 (30)	23 (30)	6 (32)	
Gastrointestinal tract	34 (35)	25 (32)	9 (47)	
Liver	76 (79)	61 (79)	15 (79)	
Lungs	12 (12)	9 (12)	3 (16)	
Joints and fascia	4 (4)	3 (4)	1 (5)	
Genital tract	2 (2)	2 (3)	0 (0)	
Number of involved organs or sites[a], n (%)				0.14
1	7 (7)	7 (9)	0 (0)	
2	27 (28)	24 (31)	3 (16)	
3 or more	62 (65)	46 (60)	16 (84)	
Maximum score of involved organs[a], n (%)				0.18
Score 1	22 (23)	20 (26)	2 (11)	
Score 2 (other than lungs)	26 (27)	18 (62)	8 (42)	
Score 2 (lungs)	6 (6)	4 (5)	2 (11)	
Score 3	42 (44)	35 (45)	7 (37)	
Severity at onset, n (%)				0.023
Mild	20 (21)	20 (26)	0 (0)	
Moderate	53 (55)	39 (51)	14 (74)	
Severe	23 (24)	18 (23)	5 (26)	
Severity at peak, n (%)				0.17
Mild	12 (13)	12 (16)	0 (0)	
Moderate	39 (41)	29 (38)	10 (53)	
Severe	45 (47)	36 (47)	9 (47)	
Platelet count at cGVHD onset, n (%)				0.002
$100 \times 10^3/\mu L$ or more	65 (68)	58 (75)	7 (37)	
Less than $100 \times 10^3/\mu L$	31 (32)	19 (25)	12 (63)	
Eosinophil count at cGVHD onset, n (%)				0.010
Less than 500/μL	68 (71)	50 (65)	18 (95)	
500/μL or more	28 (29)	27 (35)	1 (5)	
Systemic corticosteroids at cGVHD onset, n (%)				<0.001
Not received	63 (66)	61 (79)	2 (11)	
Received	33 (34)	16 (21)	17 (89)	

cGVHD chronic graft-versus-host disease

[a] Data evaluated at peak clinical worsening are shown

[b] The sum of the number per involved site is not equal to the number of evaluable patients, because the involvement of more than one organ can occur in a single patient. Accordingly, the sum of percentage among the total number of patients does not equal to one hundred

contrast, duration of IST was neither affected by NIH cGVHD subcategory nor by its severity.

While cGSS has been frequently used as a study endpoint to describe the mortality attributable to cGVHD-associated organ dysfunction, there have been no established early surrogates that help to guide the clinical management of patients with evidence of ongoing cGVHD. Given that the historic limited/extensive grading system is not a useful predictor for the severity of organ involvement in terms of mortality risk, several studies have attempted to develop